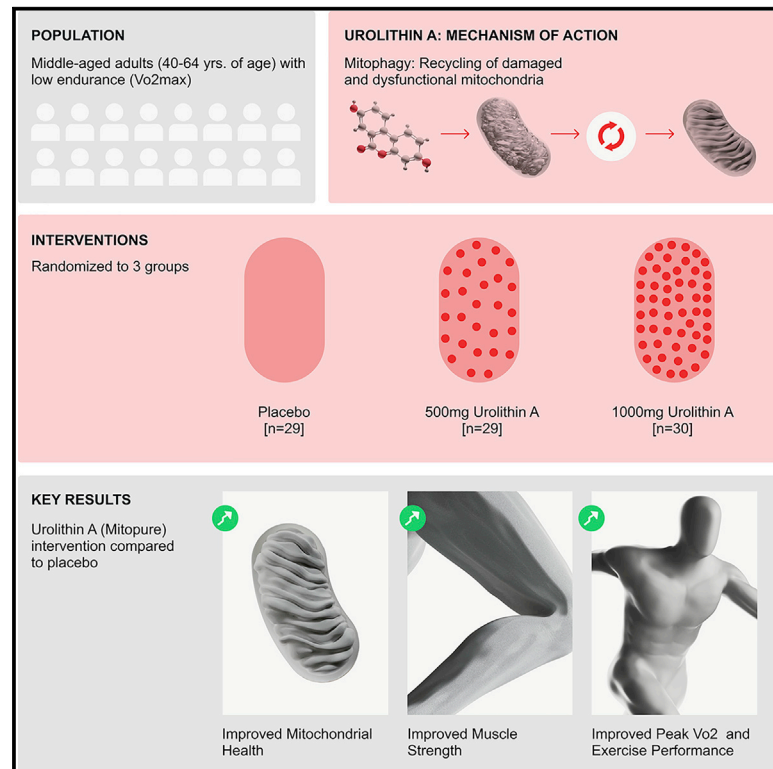Article

Urolithin A improves muscle strength, exercise performance, and biomarkers of mitochondrial health in a randomized trial in middle-aged adults

Graphical abstract

Authors
Anurag Singh, Davide D'Amico,
Pénélope A. Andreux, ...,
Patrick Aebischer, Johan Auwerx,
Chris Rinsch

Correspondence
asingh@amazentis.com

In brief
Singh et al. investigate the impact of oral supplementation with Urolithin A, a gut microbiome postbiotic known to activate mitophagy, in a randomized clinical trial in middle-aged adults. Results show that supplementation results in improvements in muscle strength and exercise-performance measures along with an impact on mitochondrial biomarkers.

Highlights

- Oral supplementation with Urolithin A increases muscle strength

- High dose of Urolithin A positively impacts exercise-performance measures

- An increase in mitophagy proteins in human skeletal muscle observed in parallel

- Supplementation is safe and increases circulating levels of Urolithin A

CellPress

Article

Urolithin A improves muscle strength, exercise performance, and biomarkers of mitochondrial health in a randomized trial in middle-aged adults

Anurag Singh,[1,5,6,*] Davide D'Amico,[1,5] Pénélope A. Andreux,[1] Andréane M. Fouassier,[1] William Blanco-Bose,[1] Mal Evans,[2] Patrick Aebischer,[3] Johan Auwerx,[4] and Chris Rinsch[1]

[1]Amazentis SA, EPFL Innovation Park, Bâtiment C, 1015 Lausanne, Switzerland
[2]KGK Science, 255 Queens Avenue #1440, London, ON N6A 5R8, Canada
[3]Ecole Polytechnique Fédérale de Lausanne, 1015 Lausanne, Switzerland
[4]Laboratory of Integrative Systems Physiology, Ecole Polytechnique Fédérale de Lausanne, 1015 Lausanne, Switzerland
[5]These authors contributed equally
[6]Lead contact
*Correspondence: asingh@amazentis.com
https://doi.org/10.1016/j.xcrm.2022.100633

SUMMARY

Targeting mitophagy to activate the recycling of faulty mitochondria during aging is a strategy to mitigate muscle decline. We present results from a randomized, placebo-controlled trial in middle-aged adults where we administer a postbiotic compound Urolithin A (Mitopure), a known mitophagy activator, at two doses for 4 months (NCT03464500). The data show significant improvements in muscle strength ($\sim$12%) with intake of Urolithin A. We observe clinically meaningful improvements with Urolithin A on aerobic endurance (peak oxygen oxygen consumption [VO_2]) and physical performance (6 min walk test) but do not notice a significant improvement on peak power output (primary endpoint). Levels of plasma acylcarnitines and C-reactive proteins are significantly lower with Urolithin A, indicating higher mitochondrial efficiency and reduced inflammation. We also examine expression of proteins linked to mitophagy and mitochondrial metabolism in skeletal muscle and find a significant increase with Urolithin A administration. This study highlights the benefit of Urolithin A to improve muscle performance.

INTRODUCTION

There are currently no effective interventions to counteract age-associated muscle decline.[1,2] While a gradual decline in muscle mass and strength with aging is natural, environmental factors such as diet and exercise dictate the trajectory of the decline.[3,4] Exercise and healthy nutrition are the primary interventions to prevent and manage age-associated decline in muscle health and metabolic diseases. Unfortunately, exercise regimes require high levels of adherence, which can be difficult to maintain.[5,6]

Mitochondrial dysfunction is a hallmark of aging and is intricately linked to age-related deterioration of skeletal muscle.[7] Studies associate impaired mitochondrial function with slow walking speed, muscle fatigue, loss of strength, and, ultimately, the development of sarcopenia.[8–10] Improving mitochondrial health is therefore a viable strategy to improve muscle health. Exercise has been shown to activate mitophagy, i.e., the removal and recycling of dysfunctional mitochondria, and to promote mitochondrial biogenesis.[11–13] To date, nutritional interventions have focused on stimulating anabolic pathways via protein supplementation. Stimulating mitophagy to reverse mitochondria dysfunction linked to aging represents a novel nutritional approach to address age-associated muscle and cellular health declines.

Urolithin A (UA) is a gut-microbiome-derived postbiotic metabolite of ellagitannins, polyphenolic compounds present in foods such as pomegranate, berries, and walnuts.[14–16] UA administration has been shown to induce mitophagy and mitochondrial function in pre-clinical models of aging and disease. At the physiological level, UA improved muscle function in nematodes,[17] young rodents,[17,18] old mice,[17] and muscle-wasting disorders such as Duchenne muscle dystrophy (DMD).[19] Other health benefits of UA were seen in age-associated diseases such as cardiac[20,21] and neurodegenerative disorders[22] and osteoarthritis,[23] as well as in inflammatory bowel diseases[24] and acute kidney injury.[25–27] From a clinical translational perspective, UA has been shown to be safe and bioavailable in humans and to enhance mitochondrial gene expression in the skeletal muscle and improve cellular health after a 4-week oral administration in sedentary older adults.[28] A recent randomized clinical trial in older adults also demonstrated improvements in muscle endurance with long-term UA intake.[29]

The current study was designed as a proof-of-concept investigation of the efficacy of long-term oral supplementation with UA on physiological endpoints in middle-aged adults. A battery of clinical and physiological outcomes linked to
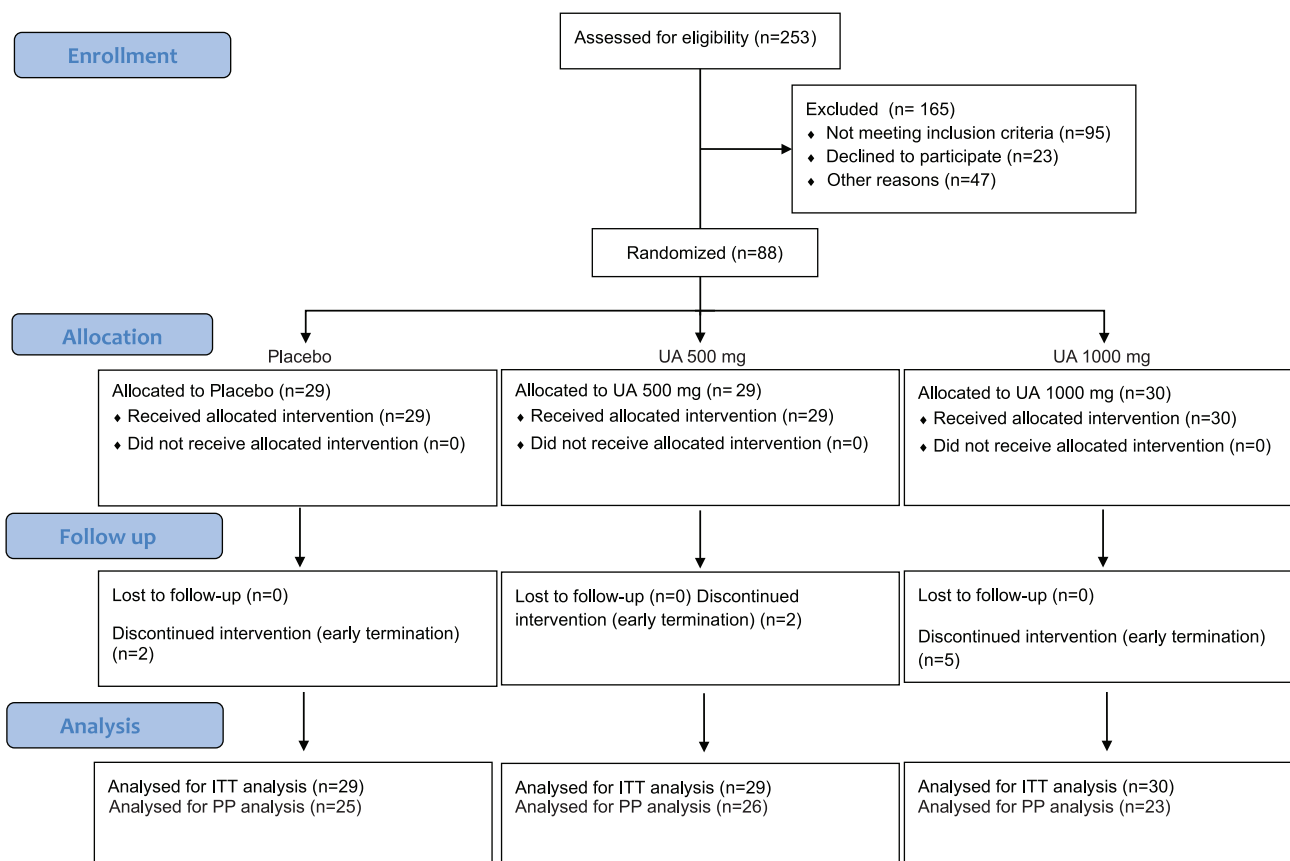
Figure 1. CONSORT diagram of participant inclusion through the clinical study
The ATLAS study was a single-center, randomized, double-blind, placebo-controlled interventional clinical trial (ClinicalTrials.gov: NCT03464500) performed in untrained, overweight, middle-aged subjects (n = 88). Subjects (253) were screened during the course of the study from a single study site. From these, eighty-eight participants that met the study inclusion and exclusion criteria were randomized in the trial. Subjects were randomized to either placebo (n = 29) or 500 (n = 29) or 1,000 mg (n = 30) doses of UA intervention. The total study duration was 4 months. Nine subjects did not complete the study (n = 9 dropouts), whereas seventy-nine (n = 79) subjects successfully completed the trial duration. All randomized subjects were included in the intent-to-treat (ITT) study population (i.e., study population consisting of all randomized participants). Dietary recall questionnaires revealed no major changes in diet during the course of the study, and the subjects did not receive any additional exercise regimen. Five subjects with low compliance were excluded from the per-protocol (PP) population (n = 74; i.e., including participants with >80% compliance and completing all study visits).

muscle strength, exercise tolerance, and physical performance were employed to study the most responsive functional endpoints to power future confirmatory clinical studies with UA. The study population consisted of untrained adults between 40 and 64 years of age. In addition, subjects were screened on the criteria of being overweight and having low physical endurance (i.e., maximum oxygen consumption [VO_{2max}] <35 kg/mL/min). A 4-month intervention period was selected as the minimal time period to start detecting an impact on physical-performance- and muscle-function-related study endpoints based on guidelines and recommendations of expert groups on clinical trials focused on muscle function.[30] Plasma samples were collected to assess the impact of UA on metabolites and cytokines associated with cellular health. Skeletal-muscle biopsies were employed to analyze UA's effects on muscle transcriptome and proteome and validate its impact on proteins linked to mitochondrial health.

RESULTS

Study participant demographics

In this randomized, double-blind, placebo-controlled study (ATLAS), 253 participants were screened. Eighty-eight subjects that successfully met all screening inclusion and exclusion criteria were randomized (Figure 1). All participants were included in the intent-to-treat (ITT) study population. Participants were deemed healthy as determined by their vital signs, anthropometric measures, and absence of any chronic medical condition. The average age of participants in the different groups was similar: 51.03 ± 7.16 years in UA 500 mg group versus 52.07 ± 5.56 years in UA 1,000 mg group versus 54.38 ± 6.48 years in the placebo group. Body mass index (BMI) across the different groups was comparable at baseline (29.52 ± 2.82 kg/m^2 in UA 500 mg groups versus 28.91 ± 2.89 kg/m^2 in UA 1,000 mg group versus 29.30 ± 2.55 kg/m^2 in the placebo group). In addition, the interventional groups were well balanced for baseline endurance

Table 1. Study-participant demographics

Population demographic characteristics: ITT population

	Placebo (n = 29)	500 mg UA (n = 29)	1,000 mg UA (n = 30)	Between group p value*
Age (years) (mean ± SD)	54.38 ± 6.42	51.03 ± 7.16	52.07 ± 5.56	0.132
Gender (n [%])				0.756
Female (%)	20 (69.00)	18 (62.10)	18 (60)	
Male (%)	9 (31.00)	11 (37.90)	12 (40)	
Weight (kg)	81.69 ± 9.44	82.93 ± 12.09	81.52 ± 11.45	0.868
Ethnicity	Western European White (n = 21; 70%); others (n = 8; 30%)	Western European White (n = 23; 79.3%); others (n = 6; 20.7%)	Western European White (n = 22; 75.9%); others (n = 8; 20.7%)	0.696
BMI (kg/m^2) (>25 kg/m^2)	29.30 ± 2.55	29.52 ± 2.82	28.91 ± 2.89	0.667
Systolic blood pressure (mmHg) (mean ± SD)	123.71 ± 11.92	124.78 ± 11.40	125.52 ± 10.24	0.824
Diastolic blood pressure (mmHg) (mean ± SD)	79.03 ± 8.68	78.41 ± 6.92	80.10 ± 7.25	0.694
Heart rate (bpm) (mean ± SD)	65.74 ± 9.61	67.60 ± 7.24	67.92 ± 8.56	0.575
V_{O2max} (mL/kg/min)	23.09 ± 4.76	23.94 ± 4.80	23.27 ± 5.92	0.806

Eighty-eight subjects that successfully met all screening inclusion and exclusion criteria were randomized. The three different study groups were well balanced on age, gender, and physical characteristics. The average age of participants was similar: 51.03 + 7.16 years in UA 500 mg group versus 52.07 + 5.56 years in UA 1,000 mg group versus 54.38 + 6.48 years in the placebo group. Body mass index (BMI) across the different groups was comparable at baseline (29.52 + 2.82 kg/m^2 in UA 500-mg groups versus 28.91 + 2.89 kg/m^2 in UA 1,000-mg group versus 29.30 + 2.55 kg/m^2 in the placebo group). Interventional groups were also well balanced for baseline endurance (VO$_{2max}$ in 500-mg group at 23.94 + 4.80 mL/kg/min versus 23.27 + 5.92 mL/kg/min in the UA 1,000 mg group versus 23.09 + 4.76 mL/kg/min in the placebo group) and vital signs.

(VO$_{2max}$ in the 500 mg group at 23.94 ± 4.80 mL/kg/min versus 23.27 ± 5.92 mL/kg/min in the UA 1,000 mg group versus 23.09 ± 4.76 mL/kg/min in the placebo group). There was a higher proportion of female participants (∼2:1; females:males) in each intervention group, and participants were predominantly of Western European ethnicity (Table 1). There were no significant between-groups differences in baseline vital signs (heart rate, blood pressure, body weight).

Long-term UA oral administration is safe and well tolerated

UA was found to be safe and well tolerated during the 120-day (4-month) supplementation period at both doses. A total of 102 post-emergent adverse events (AEs) were reported by a total of 45 participants. Of these, 42 AEs were reported by 17 participants in the placebo group, 24 reported by 13 participants in the UA 500 mg group, and 36 by 15 participants in the UA 1,000 mg group (Table S1). AEs were diverse, with a slightly greater proportion of musculoskeletal and connective tissue AEs, mostly linked to the muscle-biopsy procedure conducted at the start and end of the study intervention in a sub-group of study participants. There were no significant changes between UA groups and the placebo group on a battery of safety tests such as vital signs, blood-biochemistry parameters, hematology, and urinalysis.

UA oral administration significantly improves leg muscle strength at both doses

Muscle-strength measures were positively impacted across the different doses of UA tested (see also Table 2). Subjects supplemented with both 500 and 1,000 mg of UA showed statistically significant increases in leg muscle strength as evaluated by iso-kinetic Biodex dynamometer strength testing at baseline and end of the study. Average peak torque in the hamstring skeletal muscle was significantly increased in both UA 500 mg (+12%, p = 0.027 compared with placebo) and UA 1,000 mg groups (+9.8%, p = 0.029 compared with placebo; Figure 2A). Maximum torque during knee flexion was also significantly improved at both 500 mg UA (+10.6%, p = 0.017 compared with placebo) and 1,000 mg UA doses (+10.5%, p = 0.022 compared with placebo; Figure 2B). Participants taking the placebo had significant within-group decreases (-9.8% for average torque, p = 0.008, and -9.3% for maximum torque, p = 0.009). UA supplementation induced positive, although non-significant, improvements in the average peak torque of the quadriceps muscle (UA 500 mg: +2.3%, UA 1,000 mg: +4.7%, placebo: -2.5%, p = 0.26 between groups; Figure S1A) and in maximum torque measurement for knee extension (UA 500 mg: +2.1%, UA 1,000 mg: +5.5%, placebo: -3.3%, p = 0.18 between groups; Figure S1B). Hand-grip strength was also evaluated between the groups. Although the change from baseline was not statistically different, the 1,000 mg UA group showed a trend for a within-group improvement (5.1% improvement from baseline, p = 0.08; Figure 2C). Lean body mass evaluated via dual-energy X-ray absorptiometry (DEXA) and total fat mass (Figure S1D) were unchanged across groups after 4 months of supplementation (Figure S1C).

Impact of UA supplementation on exercise performance and aerobic endurance

A submaximal incremental exercise tolerance test was employed to assess the impact of UA on exercise-performance

Table 2. UA administration improves muscle and physical performance after 4 months

Endpoint		Placebo, %	500 mg UA, %	1,000 mg UA, %
Muscle-strength testing	hamstring average peak torque	-9.8[c]	12[a]	9.8[a]
	hamstring max. torque flexion	-9.3[c]	10.6[a,d]	10.5[a,c]
	quadriceps average peak torque	-2.5	2.3	4.7
	quadriceps max. torque extension	-3.3	2.1	5.5
	hand-grip strength	2.4	4.6	5.1[d]
Aerobic-endurance exercise testing	peak power output	0.7	4.3	3.7
	peak VO_2	-1.1	1.6	10.2[b,c]
	VO_{2max} (predicted)	4.5	-0.8	14.3[b,c]
	cycling distance	-2	6.8	15[b,c]
	time to fatigue	-5.6	3.8	3.7
	Borg rating of perceived exertion (lower scores = better)	6.7	-2.5	-3.9
Physical performance	6-min walk distance	-0.1	-0.2	7[b,c] (33.4 m)
	gait speed	-0.2	-0.2	7[b,c]
DXA (body composition)	total lean mass	-0.7	0.1	-1
	total fat mass	0.4	0.9	-1.2

Compared with the placebo group, the groups receiving UA exhibited significant improvements in leg muscle strength. The higher-UA-dose group exhibited clinically meaningful improvements on aerobic endurance (peak VO_2) and physical performance (6MWT) compared with low-UA-dose and placebo groups. Body composition was not changed across all groups during the study intervention.
[a] $p \leq 0.05$ compared with placebo.
[b] $p \geq 0.05$, but <0.10 compared with placebo.
[c] $p \leq 0.05$ within-group compared from baseline.
[d] $p \geq 0.05$, but <0.10 within group compared from baseline.

measures. Aerobic endurance measures linked to endurance and power such as peak power output (PPO) and peak VO_2, along with predicted VO_{2max}, were assessed at the start, midpoint (2 months of intervention), and end (4 months of intervention) of study. No significant change in PPO, the pre-specified primary endpoint of the study, was observed when comparing UA-supplemented groups with the placebo group (Figure 2E). However, both UA-supplemented groups showed non-significant increases of ~4% in PPO from baseline, while the placebo group remained unchanged. Supplementation with the UA 1,000 mg dose led to a statistically significant within-group increase (p < 0.01) in physical performance parameters, peak VO_2 (Figures 2D and S2A: Table 2) and estimated VO_{2max} (Figure S2B; Table 2), at both the intermediate 2-month visit (day 60) and at the end of the 4-month study intervention (day 120) compared with baseline. A non-significant trend in favor of the UA intervention (p = 0.058) was observed when comparing the UA 1,000 mg group with the placebo group for both peak VO_2 and estimated VO_{2max}. In addition, the total cycling distance increased from baseline to end of study in the 1,000 mg UA intervention group (+15%, p = 0.03 at the end-of-study within group compared with baseline; Table 2; Figure S2C), as did the time to fatigue during the exercise test (Table 2). We next investigated the impact on walking distance and gait speed following supplementation by applying the 6-min walk test (6MWT).[31,32] The UA 1,000 mg dose group showed a significant within-group increase from baseline (p = 0.008) in walking ability during the 6MWT at 4 months (p = 0.098 compared with placebo; Figure 2F; Table 2). Distance traveled increased by a mean of 33.43 m. This is note-

worthy, as such distance exceeds current estimates for clinically important differences in older adults (>30 m).[31,32] Participants in the placebo or the low-dose UA group did not show changes in the 6MWT. Similarly, gait speed improved only in the 1,000 mg UA intervention group from baseline to end of study (p = 0.004; Figure S2D; Table 2).

UA is bioavailable and induces markers of improved cellular health in the plasma
Plasma samples were collected from study participants to assess UA bioavailability and to investigate the impact of UA on surrogate biomarkers of mitochondrial and cellular health. We detected high levels of parent UA and its conjugated forms, UA-glucuronide and -sulfate (Figure 3A), 4 months after administration of UA at both doses compared with baseline. UA plasma levels achieved were consistent to those measured in the first-in-human trial with UA in older adults and suggested an excellent compliance by the study participants. Of note, only a minority of participants (~15%) showed circulating plasma UA levels at baseline prior to the start of the study intervention (Figure S3A). This is line with the reported range and variability of natural UA producers in healthy populations.[28] We next assessed whether beneficial effects of UA on muscle function translated into surrogate plasma biomarkers of health. First, we measured plasma levels of acylcarnitines, lipid molecules whose downregulation indicates improved fatty-acid oxidation.[33] Acylcarnitines were reduced in the UA 500 mg group and middle- to long-chain acylcarnitines were the most downregulated species (Figure 3B), as reported in previous clinical studies.[28,29] No changes occurred in
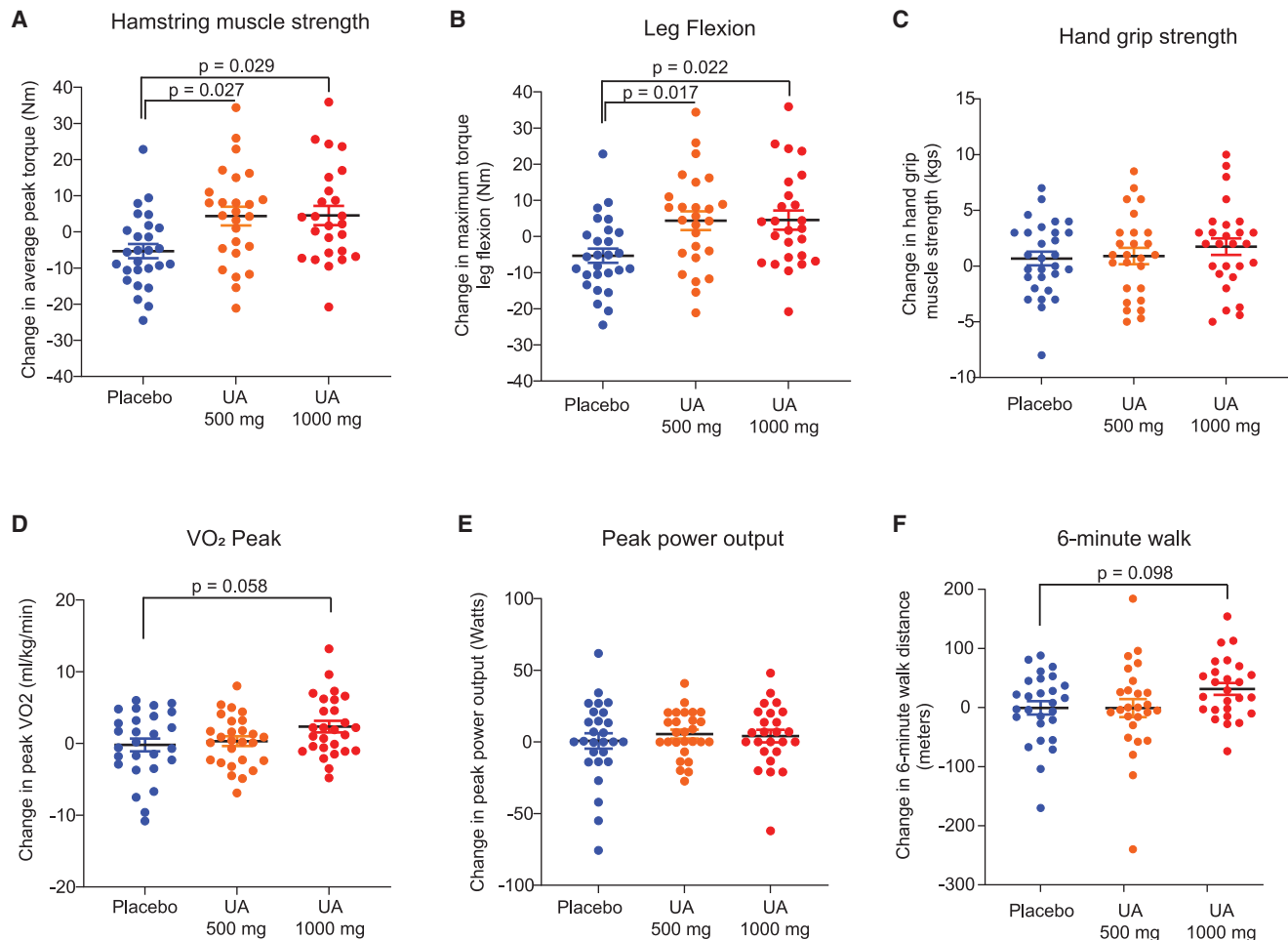
Figure 2. Urolithin A oral administration significantly improves leg muscle strength and impacts aerobic endurance in middle-aged adults

(A) At baseline and end-of-study visits, maximum strength values were calculated as the mean of the five peak torque scores (five reciprocal concentric isokinetic contractions with maximum effort) in nm for hamstring and as the one maximum score in nm for knee flexion.

(B) UA significantly improved hamstring leg muscle strength at both doses (p = 0.027 compared with placebo for 500 mg UA dose; p = 0.029 compared with placebo for 1,000 mg dose).

(C) Hand-grip strength was evaluated via hand-held dynamometry (5.1% improvement from baseline in 1,000 mg UA dose, p = 0.08).

(D) UA 1,000 mg supplementation led to significant within-group (p < 0.01; p = 0.058 compared with placebo) increases in peak VO_2.

(E) UA-supplemented groups showed non-significant increases of ~4% increase in peak power output from baseline.

(F) UA 1,000 mg dose group showed a significant within-group increase from baseline in walking distance during the 6MWT at the end-of-study visit (p ≤ 0.008).

the UA 1,000 mg cohort (Figure 3B), suggesting a possible time/duration effect of UA on this plasma biomarker.

C-reactive protein (CRP) is a well-established plasma biomarker of inflammation linked to aging[34,35] and high BMI.[36] As expected, middle-aged overweight ATLAS participants showed high average plasma CRP concentrations (approximately 3 mg/L; Figure S3B), which is associated with moderate to high risk of age-related chronic diseases.[34,35] Administration of UA reduced plasma CRP levels at both doses, with results statistically significant at the 1,000 mg dose (Figure 3C). UA also led to an overall reduction of some pro-inflammatory cytokines, such as interferon gamma (IFN-γ), interleukin-1 beta (IL-1β), and tumor necrosis factor alpha (TNF-α) (Figure 3D). Average baseline levels of these pro-inflammatory cytokines were low in this population. For several subjects, IL-1β values were below

the limit of detection. Despite this limitation, combined data from both CRP and inflammatory cytokines suggest a mild anti-inflammatory effect of UA at the systemic level. Altogether, these results indicate that UA-mediated improvement of muscle function associates with both enhanced mitochondrial efficiency and reduced inflammation.

UA induces a signature of improved cellular health in the skeletal muscle

To assess the impact of UA on muscle health at the molecular level, we analyzed transcriptomic changes in the *vastus lateralis* skeletal muscle collected at the start and end of the intervention period in the study participants. Gene set enrichment analysis (GSEA) identified pathways related to mitochondria (Figure 4B), ribosomal translation (Figure 4C), and muscle contraction
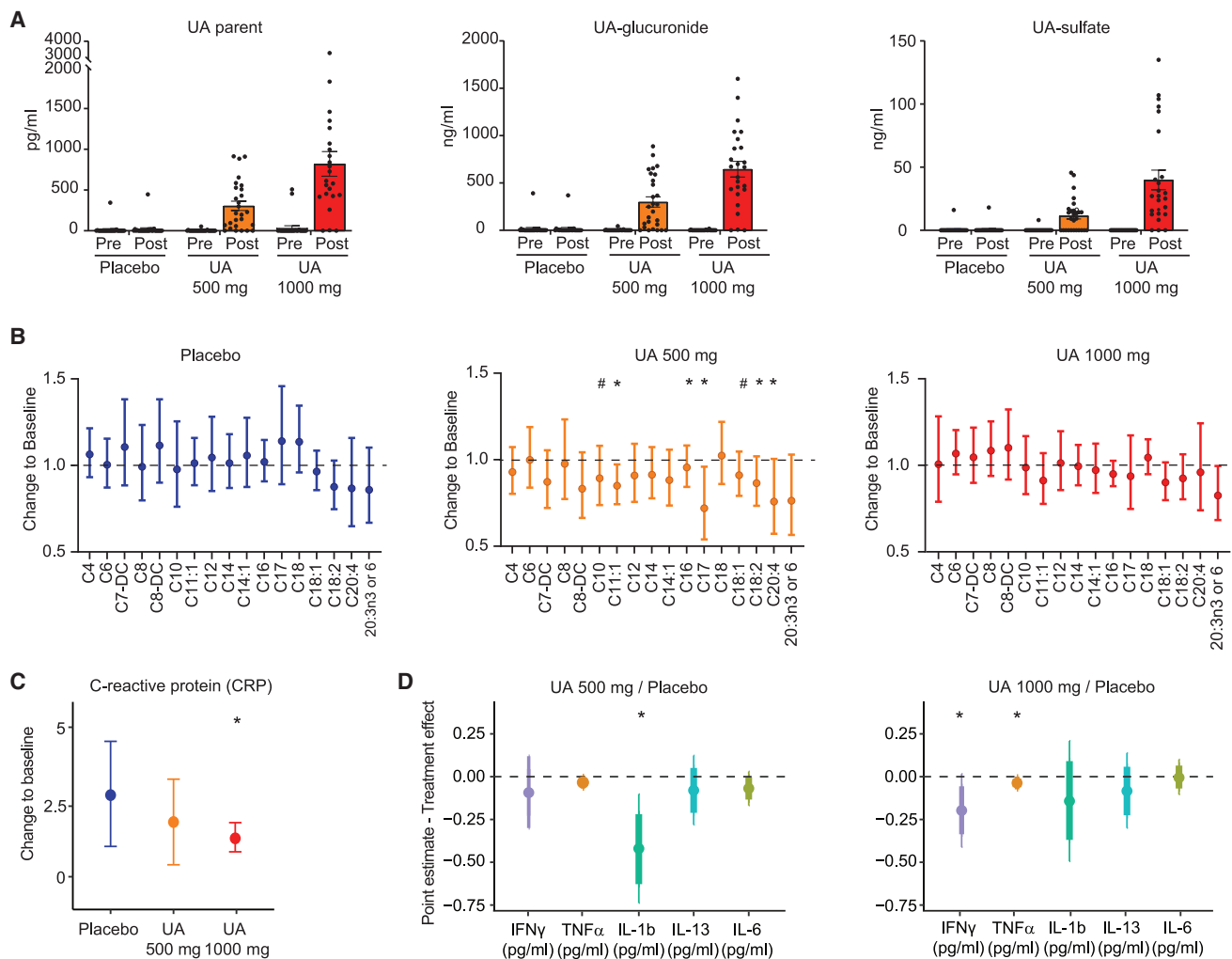
Figure 3. Effect of Urolithin A on systemic biomarkers of mitochondrial health and inflammation

(A) Dose-dependent increase in plasma UA (left), UA-glucuronide (middle), and UA-sulfate (right) plasma levels comparing baseline with the last day of the 4-month treatment period for placebo, UA 500 mg, and UA 1,000 mg doses (n = 27, placebo and UA 500 mg; n = 25, UA 1,000 mg). Data represent mean ± SEM. *p < 0.0001, after one-way ANOVA.

(B) Change in plasma levels of acylcarnitines comparing end of treatment with baseline (n = 27, placebo and UA 500 mg; n = 25, UA 1,000 mg; biologically independent samples). Data represent geometric mean ± 95% confidence interval. #0.05 < p < 0.15; *p < 0.05; after a two-way, repeated-measures ANOVA.

(C) Ratio of plasma levels of C-reactive protein (CRP) comparing end of treatment with baseline (n = 27, placebo; n = 26, UA 500 mg; n = 25, UA 1,000 mg; biologically independent samples). Data represent mean ± 95% confidence interval. *p < 0.05, after an ANCOVA model.

(D) Effect of UA 500 or UA 1,000 mg versus placebo on change to baseline plasma levels of the indicated cytokines (log10-transformed data). *p < 0.05, after an ANCOVA model.

(Figure 4D) that were significantly enriched after UA administration at the 500 mg dose (Figures 4A and S4A–S4C). The activation of mitochondrial gene sets reproduced results previously observed in muscle biopsies from the UA first-in-human study in the elderly.[28] GSEA for UA at 1,000 mg did not show significantly enriched pathways, suggesting a limited impact of UA on muscle transcriptome at this dose and time point (Figure 4A).

Biological changes occurring in the muscle are often more robust at protein than mRNA levels, as observed during muscle aging[37,38] and after physical exercise.[37,39] Therefore, we investigated the effect of UA on skeletal-muscle proteome by untargeted proteomics (Figure S5A). We analyzed proteins signifi-

cantly induced by UA but not placebo (Figure 5A). Pathways specifically enriched by UA supplementation at both doses were related to glycogen metabolism and included the glycogen debranching enzyme AGL and the myophosphorylase PYGM (Figure S5B; Table S2). Notably, these proteins are among the most significantly downregulated in the slow-twitch fiber with human aging.[40] These data suggest that UA promotes the mobilization of glucose molecules to enhance muscle metabolism.

In the proteomic analysis, the most significantly enriched pathway induced in the UA 500 mg group was "Parkin-mediated ubiquitin and proteasomal systems" (Figures 5B and S5C). This pathway contains ubiquitin-conjugating enzymes (UBEs) and
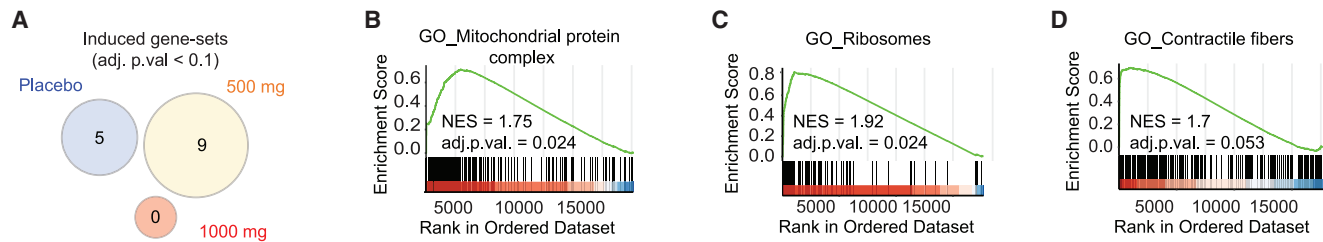
Figure 4. Impact of Urolithin A intake on human skeletal muscle transcriptome

(A) Venn diagram summarizing gene set enrichment analysis (GSEA) results from RNA-seq data in *vastus lateralis* skeletal muscle. Data represent gene sets upregulated with an adjusted p value <0.1 in subjects treated with placebo or with UA at 500 and 1,000 mg for 4 months compared with baseline.

(B–D) GSEA plots of the three most significant Gene Ontology (GO) pathways significantly enriched specifically in UA 500 mg group: GO_Mitochondrial protein complex (B), GO_Cytosolic Ribosome (C), and GO_Contractile fiber (D). Significant gene sets for the placebo group were filtered out to identify treatment-specific pathways. NES, normalized enriched score.

proteasomal components (PSMs) (Figure S5D; Table S2), which are required for Parkin-mediated degradation of dysfunctional mitochondria and damaged proteins. Enzymes such as UBE2N and UBE2R2 were previously shown to be essential for PINK1/Parkin-mediated mitophagy.[41,42] A trend toward the increase in these mitophagy-related proteins was observed also at the 1,000 mg dose (Figure S5D). Protein levels of the PINK1/Parkin-independent mitophagy regulator BNIP3 decreased in the 1,000 mg cohort (Figure S5E; Table S2), indicating a specific effect of UA on the PINK1/Parkin-mediated mitophagy axis. Top pathways enriched at the 1,000 mg dose were associated with improved mitochondrial metabolism (Figures 5C and S6A) and included proteins related to the mitochondrial tricarboxylic acid (TCA) cycle, fatty-acid oxidation, electron transport chain (ECT), and oxidative phosphorylation (OXPHOS) (Figure S6B; Table S2). Several of these mitochondrial proteins were upregulated by UA in a dose-dependent manner (Figure S6C). Among proteins indicative of mitochondria content, TOMM20 increased in the UA 1,000 mg group, although not significantly, while VDAC levels remained unchanged in all cohorts (Figure S6C; Table S2). No change was observed for proteins related to mitochondrial remodeling, such as MFN1, MFN2, DRP1, and OPA1 (Figure S6C; Table S2). Changes in mitochondrial proteome were not influenced by a switch in muscle-fiber-type composition, since the "muscle fiber ratio"[43] comparing fast- over slow-twitch fibers remained unaltered (Figure S6D).

To validate changes induced by UA on proteins related to mitophagy and mitochondrial function, we performed targeted western blot analysis on muscle-biopsy samples from the same study subjects. Targeted immunoblotting of UBE2N confirmed its increase with UA at 500 mg when comparing post- with pre-treatment (Figures S7A and S7B). At the same 500 mg dose, UA also increased levels of phospho-Parkin (Ser65), the fraction of active Parkin translocated on mitochondria and phosphorylated by PINK1 upon mitophagy activation (Figures 5D, 5E, and S7C). This supports the proteomics data indicating that UA activates PINK1/Parkin-mediated mitophagy in the human skeletal muscle.

Western blot further showed a dose-dependent increase in protein levels of complex I, II, and III OXPHOS proteins following UA supplementation. No significant changes occurred in the placebo group (Figures 5D, 5F, and S6D).

Finally, UA induced a mild increase in muscle mitochondrial content, which was measured as a mitochondrial over nuclear DNA ratio (mtDNA/nDNA) (Figure S6E), as was also seen in a previous human study.[28]

DISCUSSION

This randomized clinical trial explored the impact of long-term oral supplementation with UA on a range of muscle-health- and physical-performance-related functional endpoints in middle-aged humans. The new study builds on findings from previously reported trials with UA in older adults that demonstrated both the biological impact of UA on mitochondrial health in skeletal muscle[28] and an improvement in muscle endurance and resistance to fatigue with long-term UA supplementation.[29] The present trial was designed to assess the benefits of UA in middle-aged adults on a range of physiological and biomarker endpoints over a longer period of 4 months. Muscle biopsies have been used for a first comprehensive analysis of mRNA and protein biomarkers modulated in humans after long-term intervention with UA.

An overweight middle-aged population with a high BMI and average physical endurance was selected (Table 1), as it is known that metabolic impairments linked to overweight or obesity status lead to mitochondrial dysfunction and accelerated muscle aging.[44] A 4-month intervention was selected as the shortest period to observe improvements on functional parameters related to muscle health, given the time required at the cellular level to remodel skeletal-muscle tissue and impact muscle strength and aerobic capacity. In comparison, studies of exercise regimens typically focus on intervention periods of 6 to 12 months to observe functional benefits on physical performance and muscle function.[5,45]

Among several positive and clinically meaningful results observed in the current study (Table 2), the most striking was the impact on leg muscle strength. We observed significantly improved lower-body muscle strength in the hamstring skeletal muscle at both doses of UA. Maintaining lower-body strength and endurance is essential for healthy aging. The relationships between muscle-strength improvements with walking ability and exercise capacity have been documented in multiple longitudinal studies of aging. Unlike muscle strength, which improved
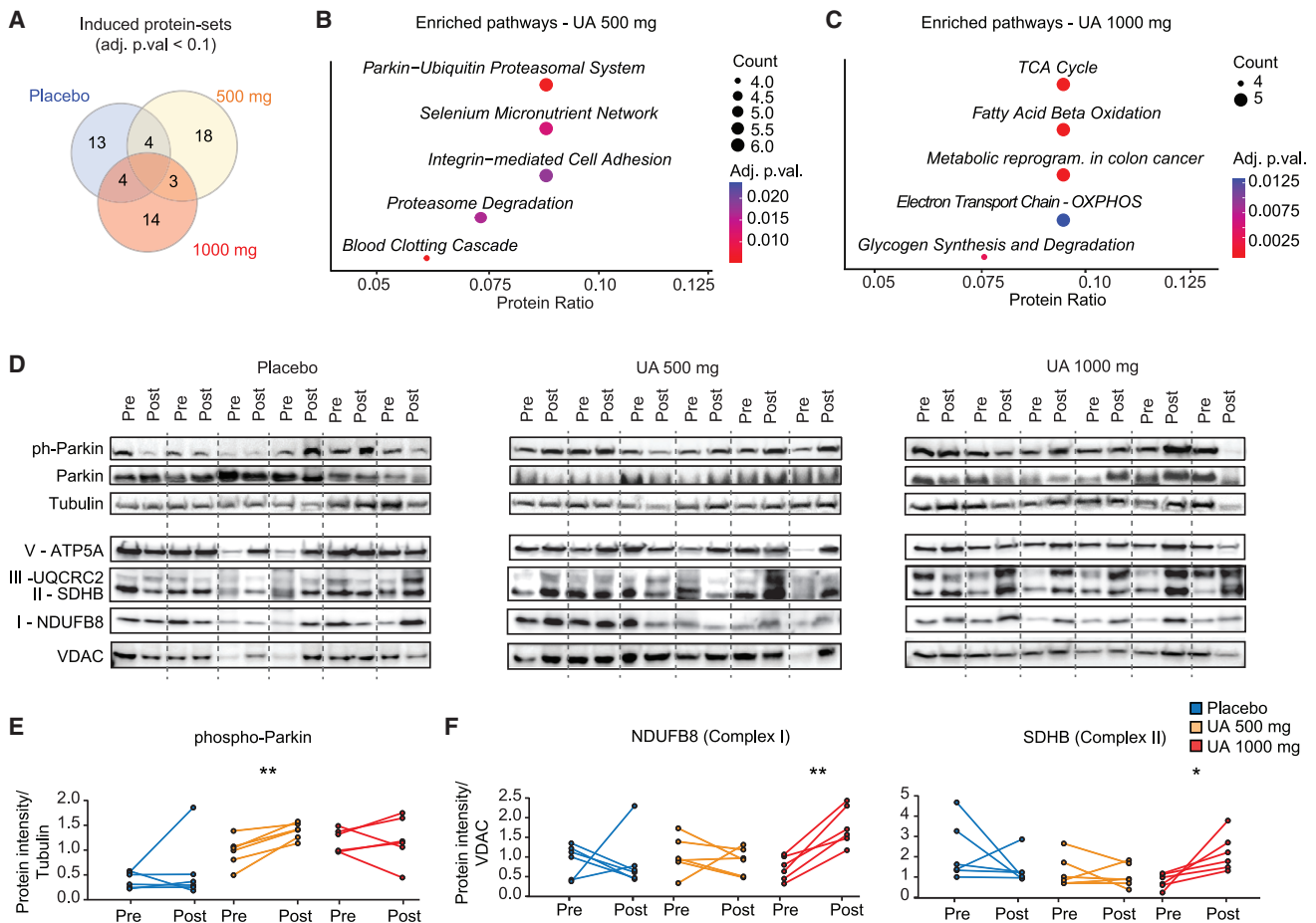
Figure 5. Urolithin A confers a proteomic signature of improved mitochondrial metabolism and mitophagy in human skeletal muscle

(A) Venn diagram summarizing pathway enrichment analysis results from proteomics data in *vastus lateralis* skeletal muscle. Data represent upregulated pathways with an adjusted p value <0.1 in subjects treated with placebo or with UA at 500 and 1,000 mg for 4 months compared with baseline.

(B and C) Dot plots showing top enriched pathways (WikiPathways 2019 Human), ranked by protein ratio, in the UA 500- (B) and UA 1,000 mg (C) groups from (A). Dot color and size indicate adjusted p value and protein count, respectively. Significant pathways for the placebo group were filtered out to identify treatment-specific pathways.

(D) Western blot analysis of protein lysates from *vastus lateralis* skeletal-muscle biopsies in subjects treated as above. For each subject, both baseline (Pre) and end-of-the-treatment (Post) samples were run, and membranes were probed for phospho-Parkin, total Parkin, and the mitochondrial proteins ATP5A (belonging to the OXPHOS complex V), UQCRC2 (complex IV), SDHB (complex II), and NDUFB8 (complex I). Tubulin and VDAC were included as markers of total and mitochondrial protein abundance, respectively. Dashed line separates samples from individual subjects. (n = 6 Pre and Post, biologically independent samples).

(E) Quantification of phospho-Parkin over Tubulin protein intensity from western blots (WBs) in (D) (n = 6). Two-sided, paired t-test.

(F) Quantification of NDUFB8 (left) and SDHB (right) protein intensity, normalized over VDAC from WBs in (D) (n = 6). *p < 0.05; **p < 0.01; two-sided, paired t test.

with both doses of UA, the results showed that only the higher dose of UA led to clinically relevant improvements in measures of physical performance (6MWT) and aerobic endurance (peak V_{O2}). This could indicate a dose-response effect with UA and also suggests that whole-body measures may require longer supplementation. It is particularly noteworthy that the group administered the high dose of UA (1,000 mg) increased their walking distance by >30 m during the 6MWT, as this reflects a clinically meaningful difference in mobility.[32]

The fact that UA treatment improved the outcomes related to physical performance in the absence of any exercise regimen is an important finding for the field. Supplementation with high (1,000 mg/d) and low (500 mg/d) doses of UA resulted in

non-significant improvements (4.30% and 3.90%, respectively) in PPO (the primary endpoint) compared with the placebo group from baseline. Although these changes are small in magnitude, they are important in the context of aging and the studied population. The ability to generate power results comes from a combination of muscle-contraction velocity, dynamic muscle force, and intrinsic bioenergetic capacity, making muscle-power production an essential component of human locomotion and function. Peak V_{O2} improved by ~10% in the high-dose UA group, with the effect already manifesting at 2-months post-UA supplementation and being maintained at 4 months. These improvements in aerobic endurance are similar to what has been previously observed in

exercise-regimen trials of the same duration in subjects with poor endurance and functional capacity.[46,47]

We also examined the effect of UA on biological pathways linked to improved muscle strength and endurance. A hallmark of muscle health is the ability to remove and recycle damaged intracellular cytosolic components.[48] Mitophagy is the process by which cells remove dysfunctional mitochondria and, in turn, regenerate functional organelles.[49] Both mitophagy and mitochondrial biogenesis decline with aging and in age-related diseases.[50] UA was shown to induce markers of mitophagy and mitochondrial function in pre-clinical models of aging.[17] In this trial, muscle RNA sequencing (RNA-seq) showed the activation of mitochondrial gene sets specifically at the UA 500 mg dose. We also observed an enrichment of gene sets related to muscle contraction and ribosome, which might suggest the activation of an anabolic response at the mRNA level. We also analyzed, for the first time, the impact of UA in skeletal muscle at the protein level. This is relevant as both aging and exercise are known to have a robust impact on muscle proteome.[37,38] Our data revealed UA to impact markers of Parkin-mediated mitophagy and to dose-dependently upregulate levels of mitochondrial TCA cycle and OXPHOS proteins. Other interventions under investigation to promote mitochondrial function in human skeletal muscle, such as nicotinamide riboside (NR), did not show changes in mitochondrial abundance or function after 4–8 weeks of supplementation, which may be on the shorter side to observe an impact.[51,52] Notably, mitochondrial proteins are upregulated by UA to an extent that is comparable to what is observed after undergoing physical exercise regimens.[53,54]

To look at UA's impact on mitochondrial health systemically, we measured plasma acylcarnitines. Reduction in acylcarnitine plasma levels is linked to enhanced mitochondrial efficiency.[55] In line with this, circulating acylcarnitines are increased during aging[56] and in conditions associated with mitochondrial dysfunction[57] while being lowered by long-term exercise.[58] Previous data in elderly subjects showed that UA supplementation reduced plasma acylcarnitines.[28,29] The current study reproduced these data after long-term administration and in a different population, albeit only at the 500 mg UA dose. These data suggest that the impact of UA on acylcarnitines might be function of the length of intervention and dosing.

Together with its benefit on mitochondrial health, UA also reduced plasma biomarkers of inflammation. The reduction of the CRP by UA is particularly relevant, as circulating CRP concentration is positively associated with an increased risk of age-related diseases and with poorer immune health.[34,35] Of note, plasma CRP levels are also inversely correlated with muscle mitochondrial oxidative capacity.[59] These biomarker data indicate how UA supplementation offers a potential dual benefit for muscle health, by improving mitochondrial function, while also acting to reduce age-related chronic inflammation, or inflamm-aging.[60] UA induction of mitophagy could potentially mediate its anti-inflammatory effect, as removing dysfunctional mitochondria reduces the production of reactive oxygen species (ROS) and the release of mtDNA and cardiolipins, known triggers of inflammatory responses.[50,61] In turn, UA-mediated reduction of inflammatory markers could contribute to blunting their negative regulation of mitochondrial biogenesis effectors,

such as PGC1a and SIRT1, thereby allowing the generation of new mitochondria.[61,62] How UA impacts both mitochondrial health and inflammation is an intriguing question that warrants in-depth mechanistic studies in more suited experimental models.

A key finding of the present study is the clinically meaningful impact of UA on improving muscle strength and positively impacting aerobic endurance and physical-performance measures such as walking distance. These findings build on previous clinical evidence with UA and its use as a nutritional intervention to support muscle health and promote healthy aging. Future confirmatory studies will focus on functional endpoints that had an impact with UA supplementation, in particular on muscle strength and aerobic endurance, and will be powered based on the findings of this proof-of-concept study.

Limitations of the study

One of the main limitations of the study is that the primary endpoint of the study, PPO, was not significantly different between the UA groups versus the placebo group. This proof-of-concept study investigated the impact of UA on muscle strength and function in middle-aged adults. Therefore, sample-size estimates and treatment effects could be estimated only based on published exercise intervention studies of longer durations in excess of 4 months.[47,63] Despite this limitation, the data obtained with this trial will help design future well-powered, confirmatory studies focused on muscle-strength and aerobic-endurance outcomes. Another limitation of the study is the finding that some biological pathways were not significantly modulated by UA at all doses. We also did not observe an overlap in pathways activated by UA when comparing RNA-seq and proteomics data. This lack of consistency could be a limitation to interpret the results. However, data could simply indicate UA's pharmacodynamics in human, with different sets of biomarkers activated by the compound at either the mRNA or the protein level depending on dose and duration of the administration. Such a model is supported by previous studies also showing that aging and exercise interventions have a different impact on transcriptome and proteome over time.[37,64]

STAR★METHODS

Detailed methods are provided in the online version of this paper and include the following:

- KEY RESOURCES TABLE
- RESOURCE AVAILABILITY
  - Lead contact
  - Materials availability
  - Data and code availability
- EXPERIMENTAL MODEL AND SUBJECT DETAILS
  - Trial design and study schedule
  - Inclusion and exclusion criteria
- METHOD DETAILS
  - Product intake and randomization
  - Compliance
  - Adverse event reporting
  - Data management and monitoring

- Lower-body (muscle strength testing) using Biodex dynamometry
- Upper-body (hand-grip) muscle strength evaluation using dynamometry
- Incremental sub-maximal exercise testing
- Dual energy X-ray absorptiometry (DXA)
- 6-min walk test (6MWT)
- Plasma collection
- Bioavailability assessment of UA
- Plasma metabolomics
- Plasma CRP and cytokine measurements
- Muscle biopsies procedure
- mRNA extraction from muscle biopsies
- Library preparation and RNA-seq
- Gene expression analysis using RNA-seq
- Gene set enrichment analysis (GSEA)
- Muscle proteomics
- Western blot analysis
- mtDNA/nuDNA analysis
- **QUANTIFICATION AND STATISTICAL ANALYSIS**
  - Clinical data
  - Plasma biomarkers
  - RNA-seq
  - Proteomics
  - mtDNA/nuDNA

REFERENCES

1. Denison, H.J., Cooper, C., Sayer, A.A., Aihie Sayer, A., and Robinson, S.M. (2015). Prevention and optimal management of sarcopenia: a review of combined exercise and nutrition interventions to improve muscle outcomes in older people. Clin. Interventions Aging 10, 859–869. https://doi.org/10.2147/cia.s55842. https://www.dovepress.com/prevention-and-optimal-management-of-sarcopenia-a-review-of-combined-e-peer-reviewed-article-CIA.

2. Kwak, J.Y., and Kwon, K.-S. (2019). Pharmacological interventions for treatment of sarcopenia: current status of drug development for sarcopenia. Ann. Geriatr. Med. Res. 23, 98–104. https://doi.org/10.4235/agmr.19.0028.

3. Siparsky, P.N., Kirkendall, D.T., and Garrett, W.E. (2014). Muscle changes in aging. Sports Health 6, 36–40. https://doi.org/10.1177/1941738113502296.

4. Goodpaster, B.H., Park, S.W., Harris, T.B., Kritchevsky, S.B., Nevitt, M., Schwartz, A.V., Simonsick, E.M., Tylavsky, F.A., Visser, M., and Newman, A.B.; for the Health ABC Study (2006). The loss of skeletal muscle strength, mass, and quality in older adults: the health, aging and body composition study. J. Gerontol. Ser. A 61, 1059–1064. https://doi.org/10.1093/gerona/61.10.1059.

5. Di Lorito, C., Long, A., Byrne, A., Harwood, R.H., Gladman, J.R., Schneider, S., Logan, P., Bosco, A., and van der Wardt, V. (2021). Exercise interventions for older adults: a systematic review of meta-analyses. J. Sport Health Sci. 10, 29–47. https://doi.org/10.1016/j.jshs.2020.06.003.

6. Kell, K.P., and Rula, E.Y. (2019). Increasing exercise frequency is associated with health and quality-of-life benefits for older adults. Qual. Life Res. 28, 3267–3272. https://doi.org/10.1007/s11136-019-02264-z.

7. López-Otín, C., Blasco, M.A., Partridge, L., Serrano, M., and Kroemer, G. (2013). The hallmarks of aging. Cell 153, 1194–1217. https://doi.org/10.1016/j.cell.2013.05.039.

8. Santanasto, A.J., Coen, P.M., Glynn, N.W., Conley, K.E., Jubrias, S.A., Amati, F., Strotmeyer, E.S., Boudreau, R.M., Goodpaster, B.H., and Newman, A.B. (2016). The relationship between mitochondrial function and walking performance in older adults with a wide range of physical function. Exp. Gerontol. 81, 1–7. https://doi.org/10.1016/j.exger.2016.04.002.

9. Coen, P.M., Jubrias, S.A., Distefano, G., Amati, F., Mackey, D.C., Glynn, N.W., Manini, T.M., Wohlgemuth, S.E., Leeuwenburgh, C., Cummings, S.R., et al. (2013). Skeletal muscle mitochondrial energetics are associated with maximal aerobic capacity and walking speed in older adults. J. Gerontol. A. Biol. Sci. Med. Sci. 68, 447–455. https://doi.org/10.1093/gerona/gls196.

10. Migliavacca, E., Tay, S.K.H., Patel, H.P., Sonntag, T., Civiletto, G., McFarlane, C., Forrester, T., Barton, S.J., Leow, M.K., Antoun, E., et al. (2019). Mitochondrial oxidative capacity and NAD+ biosynthesis are reduced in human sarcopenia across ethnicities. Nat. Commun. 10, 5808. https://doi.org/10.1038/s41467-019-13694-1.

11. Jacobs, R.A., Fluck, D., Bonne, T.C., Burgi, S., Christensen, P.M., Toigo, M., and Lundby, C. (2013). Improvements in exercise performance with high-intensity interval training coincide with an increase in skeletal muscle mitochondrial content and function. J. Appl. Physiol. 115, 785–793. https://doi.org/10.1152/japplphysiol.00445.2013.

12. Balan, E., Schwalm, C., Naslain, D., Nielens, H., Francaux, M., and Deldicque, L. (2019). Regular endurance exercise promotes fission, mitophagy, and oxidative phosphorylation in human skeletal muscle independently of age. Front. Physiol. 10, 1088. https://doi.org/10.3389/fphys.2019.01088.

13. Lo Verso, F., Carnio, S., Vainshtein, A., and Sandri, M. (2014). Autophagy is not required to sustain exercise and PRKAA1/AMPK activity but is important to prevent mitochondrial damage during physical activity. Autophagy 10, 1883–1894. https://doi.org/10.4161/auto.32154.

14. Tomás-Barberán, F.A., Gonzalez-Sarrias, A., Garcia-Villalba, R., Nunez-Sanchez, M.A., Selma, M.V., Garcia-Conesa, M.T., and Espin, J.C. (2017). Urolithins, the rescue of "old" metabolites to understand a "new" concept: metabotypes as a nexus among phenolic metabolism, microbiota dysbiosis, and host health status. Mol. Nutr. Food Res. 61, 1500901. https://doi.org/10.1002/mnfr.201500901.

15. Espín, J.C., Larrosa, M., García-Conesa, M.T., and Tomás-Barberán, F. (2013). Biological significance of Urolithins, the gut microbial ellagic acid-derived metabolites: the evidence so far. Evidence-Based Complement. Altern. Med. *2013*, e270418. https://www.hindawi.com/journals/ecam/2013/270418/.

16. D'Amico, D., Andreux, P.A., Valdes, P., Singh, A., Rinsch, C., and Auwerx, J. (2021). Impact of the natural compound urolithin A on health, disease, and aging. Trends Mol. Med. *27*, 687–699. https://doi.org/10.1016/j.molmed.2021.04.009.

17. Ryu, D., Mouchiroud, L., Andreux, P.A., Katsyuba, E., Moullan, N., Nicolet-dit-Felix, A.A., Williams, E.G., Jha, P., Lo Sasso, G., Huzard, D., et al. (2016). Urolithin A induces mitophagy and prolongs lifespan in C. elegans and increases muscle function in rodents. Nat. Med. *22*, 879–888. https://doi.org/10.1038/nm.4132.

18. Xia, B., Shi, X.C., Xie, B.C., Zhu, M.Q., Chen, Y., Chu, X.Y., Cai, G.H., Liu, M., Yang, S.Z., Mitchell, G.A., et al. (2020). Urolithin A exerts antiobesity effects through enhancing adipose tissue thermogenesis in mice. PLOS Biol. *18*, e3000688. https://doi.org/10.1371/journal.pbio.3000688.

19. Luan, P., D'Amico, D., Andreux, P.A., Laurila, P.P., Wohlwend, M., Li, H., Imamura de Lima, T., Place, N., Rinsch, C., Zanou, N., and Auwerx, J. (2021). Urolithin A improves muscle function by inducing mitophagy in muscular dystrophy. Sci. Transl. Med. *13*, eabb0319. https://doi.org/10.1126/scitranslmed.abb0319.

20. Savi, M., Bocchi, L., Mena, P., Dall'Asta, M., Crozier, A., Brighenti, F., Stilli, D., and Del Rio, D. (2017). *In vivo* administration of urolithin A and B prevents the occurrence of cardiac dysfunction in streptozotocin-induced diabetic rats. Cardiovasc. Diabetol. *16*, 80.

21. Tang, L., Mo, Y., Li, Y., Zhong, Y., He, S., Zhang, Y., Tang, Y., Fu, S., Wang, X., and Chen, A. (2017). Urolithin A alleviates myocardial ischemia/reperfusion injury via Pl3K/Akt pathway. Biochem. Biophys. Res. Commun. *486*, 774–780. https://doi.org/10.1016/j.bbrc.2017.03.119.

22. Fang, E.F., Hou, Y., Palikaras, K., Adriaanse, B.A., Kerr, J.S., Yang, B., Lautrup, S., Hasan-Olive, M.M., Caponio, D., Dan, X., et al. (2019). Mitophagy inhibits amyloid-β and tau pathology and reverses cognitive deficits in models of Alzheimer's disease. Nat. Neurosci. *22*, 401–412. https://doi.org/10.1038/s41593-018-0332-9.

23. Fu, X., Gong, L.F., Wu, Y.F., Lin, Z., Jiang, B.J., Wu, L., and Yu, K.H. (2019). Urolithin A targets the PI3K/Akt/NF-κB pathways and prevents IL-1β-induced inflammatory response in human osteoarthritis: in vitro and in vivo studies. Food Funct. *10*, 6135–6146. https://doi.org/10.1039/c9fo01332f.

24. Singh, R., Chandrashekharappa, S., Bodduluri, S.R., Baby, B.V., Hegde, B., Kotla, N.G., Hiwale, A.A., Saiyed, T., Patel, P., Vijay-Kumar, M., et al. (2019). Enhancement of the gut barrier integrity by a microbial metabolite through the Nrf2 pathway. Nat. Commun. *10*, 89. https://doi.org/10.1038/s41467-018-07859-7.

25. Guada, M., Ganugula, R., Vadhanam, M., and Ravi Kumar, M.N.V. (2017). Urolithin A mitigates cisplatin-induced nephrotoxicity by inhibiting renal inflammation and apoptosis in an experimental rat model. J. Pharmacol. Exp. Ther. *363*, 58–65. https://doi.org/10.1124/jpet.117.242420.

26. Zou, D., Ganugula, R., Arora, M., Nabity, M.B., Sheikh-Hamad, D., and Kumar, M.N.V.R. (2019). Oral delivery of nanoparticle urolithin A normalizes cellular stress and improves survival in mouse model of cisplatin-induced AKI. Am. J. Physiol. Renal Physiol. *317*, F1255–F1264. https://doi.org/10.1152/ajprenal.00346.2019.

27. Jing, T., Liao, J., Shen, K., Chen, X., Xu, Z., Tian, W., Wang, Y., Jin, B., and Pan, H. (2019). Protective effect of urolithin a on cisplatin-induced nephrotoxicity in mice via modulation of inflammation and oxidative stress. Food Chem. Toxicol. *129*, 108–114. https://doi.org/10.1016/j.fct.2019.04.031.

28. Andreux, P.A., Blanco-Bose, W., Ryu, D., Burdet, F., Ibberson, M., Aebischer, P., Auwerx, J., Singh, A., and Rinsch, C. (2019). The mitophagy activator urolithin A is safe and induces a molecular signature of improved mitochondrial and cellular health in humans. Nat. Metab. *1*, 595–603. https://doi.org/10.1038/s42255-019-0073-4.

29. Liu, S., D'Amico, D., Shankland, E., Bhayana, S., Garcia, J.M., Aebischer, P., Rinsch, C., Singh, A., and Marcinek, D.J. (2022). Effect of urolithin A supplementation on muscle endurance and mitochondrial health in older adults: a randomized clinical trial. JAMA Netw. Open *5*, e2144279. https://doi.org/10.1001/jamanetworkopen.2021.44279.

30. Reginster, J.-Y., Beaudart, C., Al-Daghri, N., Avouac, B., Bauer, J., Bere, N., Bruyere, O., Cerreta, F., Cesari, M., Rosa, M.M., et al. (2021). Update on the ESCEO recommendation for the conduct of clinical trials for drugs aiming at the treatment of sarcopenia in older adults. Aging Clin. Exp. Res. *33*, 3–17. https://doi.org/10.1007/s40520-020-01663-4.

31. Perera, S., Mody, S.H., Woodman, R.C., and Studenski, S.A. (2006). Meaningful change and responsiveness in common physical performance measures in older adults. J. Am. Geriatr. Soc. *54*, 743–749. https://doi.org/10.1111/j.1532-5415.2006.00701.x.

32. Bohannon, R.W., and Crouch, R. (2017). Minimal clinically important difference for change in 6-minute walk test distance of adults with pathology: a systematic review. J. Eval. Clin. Pract. *23*, 377–381. https://doi.org/10.1111/jep.12629.

33. Schooneman, M.G., Vaz, F.M., Houten, S.M., and Soeters, M.R. (2013). Acylcarnitines. Diabetes *62*, 1–8. https://doi.org/10.2337/db12-0466.

34. Lassale, C., Batty, G.D., Steptoe, A., Cadar, D., Akbaraly, T.N., Kivimaki, M., and Zaninotto, P. (2019). Association of 10-year C-reactive protein trajectories with markers of healthy aging: findings from the English longitudinal study of aging. J. Gerontol. A. Biol. Sci. Med. Sci. *74*, 195–203. https://doi.org/10.1093/gerona/gly028.

35. Puzianowska-Kuźnicka, M., Owczarz, M., Wieczorowska-Tobis, K., Nadrowski, P., Chudek, J., Slusarczyk, P., Skalska, A., Jonas, M., Franek, E., and Mossakowska, M. (2016). Interleukin-6 and C-reactive protein, successful aging, and mortality: the PolSenior study. Immun. Ageing *13*, 21. https://doi.org/10.1186/s12979-016-0076-x.

36. Visser, M. (1999). Elevated C-reactive protein levels in overweight and obese adults. JAMA *282*, 2131. https://doi.org/10.1001/jama.282.22.2131.

37. Robinson, M.M., Dasari, S., Konopka, A.R., Johnson, M.L., Manjunatha, S., Esponda, R.R., Carter, R.E., Lanza, I.R., and Nair, K.S. (2017). Enhanced protein translation underlies improved metabolic and physical adaptations to different exercise training modes in young and old humans. Cell Metab. *25*, 581–592. https://doi.org/10.1016/j.cmet.2017.02.009.

38. Ubaida-Mohien, C., Lyashkov, A., Gonzalez-Freire, M., Tharakan, R., Shardell, M., Moaddel, R., Semba, R.D., Chia, C.W., Gorospe, M., Sen, R., et al. (2019). Discovery proteomics in aging human skeletal muscle finds change in spliceosome, immunity, proteostasis and mitochondria. eLife *8*, e49874.

39. Miller, B.F., Konopka, A.R., and Hamilton, K.L. (2016). The rigorous study of exercise adaptations: why mRNA might not be enough. J. Appl. Physiol. *121*, 594–596. https://doi.org/10.1152/japplphysiol.00137.2016.

40. Murgia, M., Toniolo, L., Nagaraj, N., Ciciliot, S., Vindigni, V., Schiaffino, S., Reggiani, C., and Mann, M. (2017). Single muscle fiber proteomics reveals fiber-type-specific features of human muscle aging. Cell Rep. *19*, 2396–2409. https://doi.org/10.1016/j.celrep.2017.05.054.

41. Geisler, S., Vollmer, S., Golombek, S., and Kahle, P.J. (2014). The ubiquitin-conjugating enzymes UBE2N, UBE2L3 and UBE2D2/3 are essential for Parkin-dependent mitophagy. J. Cell Sci *127*, 3280–3293. https://doi.org/10.1242/jcs.146035.

42. Scott, H.L., Buckner, N., Fernandez-Albert, F., Pedone, E., Postiglione, L., Shi, G., Allen, N., Wong, L.F., Magini, L., Marucci, L., et al. (2020). A dual druggable genome-wide siRNA and compound library screening approach identifies modulators of parkin recruitment to mitochondria. J. Biol. Chem. *295*, 3285–3300. https://doi.org/10.1074/jbc.ra119.009699.

43. Schiaffino, S., and Reggiani, C. (2011). Fiber types in mammalian skeletal muscles. Physiol. Rev. *91*, 1447–1531. https://doi.org/10.1152/physrev.00031.2010.

44. Bournat, J.C., and Brown, C.W. (2010). Mitochondrial dysfunction in obesity. Curr. Opin. Endocrinol. Diabetes Obes. *17*, 446–452. https://doi.org/10.1097/med.0b013e32833c3026.

45. Geirsdottir, O.G., Arnarson, A., Ramel, A., Briem, K., Jonsson, P.V., and Thorsdottir, I. (2015). Muscular strength and physical function in elderly adults 6–18 months after a 12-week resistance exercise program. Scand. J. Public Health *43*, 76–82. https://doi.org/10.1177/1403494814560842.

46. Mueller, S., Winzer, E.B., Duvinage, A., Gevaert, A.B., Edelmann, F., Haller, B., Pieske-Kraigher, E., Beckers, P., Bobenko, A., Hommel, J., et al.; OptimEx-Clin Study Group (2021). Effect of high-intensity interval training, moderate continuous training, or guideline-based physical activity advice on peak oxygen consumption in patients with heart failure with preserved ejection fraction: a randomized clinical trial. JAMA *325*, 542–551. https://doi.org/10.1001/jama.2020.26812.

47. Kitzman, D.W., Brubaker, P., Morgan, T., Haykowsky, M., Hundley, G., Kraus, W.E., Eggebeen, J., and Nicklas, B.J. (2016). Effect of caloric restriction or aerobic exercise training on peak oxygen consumption and quality of life in obese older patients with heart failure with preserved ejection fraction: a randomized clinical trial. JAMA *315*, 36. https://doi.org/10.1001/jama.2015.17346.

48. López-Otín, C., and Kroemer, G. (2021). Hallmarks of health. Cell *184*, 33–63. https://doi.org/10.1016/j.cell.2020.11.034.

49. Palikaras, K., Lionaki, E., and Tavernarakis, N. (2018). Mechanisms of mitophagy in cellular homeostasis, physiology and pathology. Nat. Cell Biol. *20*, 1013–1022. https://doi.org/10.1038/s41556-018-0176-2.

50. Sun, N., Youle, R.J., and Finkel, T. (2016). The mitochondrial basis of aging. Mol. Cell *61*, 654–666. https://doi.org/10.1016/j.molcel.2016.01.028.

51. Elhassan, Y.S., Kluckova, K., Fletcher, R.S., Schmidt, M.S., Garten, A., Doig, C.L., Cartwright, D.M., Oakey, L., Burley, C.V., Jenkinson, N., et al. (2019). Nicotinamide riboside augments the aged human skeletal muscle NAD+ metabolome and induces transcriptomic and anti-inflammatory signatures. Cell Rep. *28*, 1717–1728.e6. https://doi.org/10.1016/j.celrep.2019.07.043.e6.

52. Dollerup, O.L., Chubanava, S., Agerholm, M., Sondergard, S.D., Altintas, A., Moller, A.B., Hoyer, K.F., Ringgaard, S., Stodkilde-Jorgensen, H., Lavery, G.G., et al. (2020). Nicotinamide riboside does not alter mitochondrial respiration, content or morphology in skeletal muscle from obese and insulin-resistant men. J. Physiol. *598*, 731–754. https://doi.org/10.1113/jp278752.

53. Hussey, S.E., Sharoff, C.G., Garnham, A., YI, Z., Bowen, B.P., Mandarino, L.J., and Hargreaves, M. (2013). Effect of exercise on the skeletal muscle proteome in patients with type 2 diabetes. Med. Sci. Sports Exerc. *45*, 1069–1076. https://doi.org/10.1249/mss.0b013e3182814917.

54. Porter, C., Reidy, P.T., Bhattarai, N., Sidossis, L.S., and Rasmussen, B.B. (2015). Resistance exercise training alters mitochondrial function in human skeletal muscle. Med. Sci. Sports Exerc. *47*, 1922–1931. https://doi.org/10.1249/mss.0000000000000605.

55. McCann, M.R., George De la Rosa, M.V., Rosania, G.R., and Stringer, K.A. (2021). L-carnitine and acylcarnitines: mitochondrial biomarkers for precision medicine. Metabolites *11*, 51. https://doi.org/10.3390/metabo11010051.

56. Darst, B.F., Koscik, R.L., Hogan, K.J., Johnson, S.C., and Engelman, C.D. (2019). Longitudinal plasma metabolomics of aging and sex. Aging (Albany NY) *11*, 1262–1282. https://doi.org/10.18632/aging.101837.

57. Thompson Legault, J., Strittmatter, L., Tardif, J., Sharma, R., Tremblay-Vaillancourt, V., Aubut, C., Boucher, G., Clish, C., Cyr, D., Daneault, C., et al. (2015). A metabolic signature of mitochondrial dysfunction revealed through a monogenic form of leigh syndrome. Cell Rep. *13*, 981–989. https://doi.org/10.1016/j.celrep.2015.09.054.

58. Felder, T.K., Ring-Dimitriou, S., Auer, S., Soyal, S.M., Kedenko, L., Rinnerthaler, M., Cadamuro, J., Haschke-Becher, E., Aigner, E., Paulweber, B., and Patsch, W. (2017). Specific circulating phospholipids, acylcarnitines, amino acids and biogenic amines are aerobic exercise markers. J. Sci. Med. Sport *20*, 700–705. https://doi.org/10.1016/j.jsams.2016.11.011.

59. Zampino, M., Brennan, N.A., Kuo, P.L., Spencer, R.G., Fishbein, K.W., Simonsick, E.M., and Ferrucci, L. (2020). Poor mitochondrial health and systemic inflammation? Test of a classic hypothesis in the Baltimore Longitudinal Study of Aging. GeroScience *42*, 1175–1182. https://doi.org/10.1007/s11357-020-00208-x.

60. Franceschi, C., Garagnani, P., Parini, P., Giuliani, C., and Santoro, A. (2018). Inflammaging: a new immune–metabolic viewpoint for age-related diseases. Nat. Rev. Endocrinol. *14*, 576–590. https://doi.org/10.1038/s41574-018-0059-4.

61. Reid, A.L., and Alexander, M.S. (2021). The interplay of mitophagy and inflammation in Duchenne muscular dystrophy. Life *11*, 648. https://doi.org/10.3390/life11070648.

62. Remels, A.H.V., Gosker, H., Bakker, J., Guttridge, D., Schols, A., and Langen, R. (2013). Regulation of skeletal muscle oxidative phenotype by classical NF-κB signalling. Biochim. Biophys. Acta (Bba) - Mol. Basis Dis. *1832*, 1313–1325. https://doi.org/10.1016/j.bbadis.2013.03.018.

63. Meex, R.C.R., Schrauwen-Hinderling, V.B., Moonen-Kornips, E., Schaart, G., Mensink, M., Phielix, E., van de Weijer, T., Sels, J.P., Schrauwen, P., and Hesselink, M.K. (2010). Restoration of muscle mitochondrial function and metabolic flexibility in type 2 diabetes by exercise training is paralleled by increased myocellular fat storage and improved insulin sensitivity. Diabetes *59*, 572–579. https://doi.org/10.2337/db09-1322.

64. Tharakan, R., Ubaida-Mohien, C., Piao, Y., Gorospe, M., and Ferrucci, L. (2021). Ribosome profiling analysis of human skeletal muscle identifies reduced translation of mitochondrial proteins with age. RNA Biol. *18*, 1555–1559. https://doi.org/10.1080/15476286.2021.1875647.

65. Milburn, M.V., and Lawton, K.A. (2013). Application of metabolomics to diagnosis of insulin resistance. Annu. Rev. Med. *64*, 291–305. https://doi.org/10.1146/annurev-med-061511-134747.

66. Love, M.I., Huber, W., and Anders, S. (2014). Moderated estimation of fold change and dispersion for RNA-seq data with DESeq2. Genome Biol. *15*, 550. https://doi.org/10.1186/s13059-014-0550-8.

67. Yu, G., Wang, L.-G., Han, Y., and He, Q.-Y. (2012). clusterProfiler: an R Package for comparing biological themes among gene clusters. OMICS: A J. Integr. Biol. *16*, 284–287. https://doi.org/10.1089/omi.2011.0118.

68. Kelstrup, C.D., Bekker-Jensen, D.B., Arrey, T.N., Hogrebe, A., Harder, A., and Olsen, J.V. (2018). Performance evaluation of the Q exactive HF-X for shotgun proteomics. J. Proteome Res. *17*, 727–738. https://doi.org/10.1021/acs.jproteome.7b00602.

69. Bruderer, R., Bernhardt, O.M., Gandhi, T., Xuan, Y., Sondermann, J., Schmidt, M., Gomez-Varela, D., and Reiter, L. (2017). Optimization of experimental parameters in data-independent mass spectrometry significantly increases depth and reproducibility of results. Mol. Cell Proteomics *16*, 2296–2309. https://doi.org/10.1074/mcp.ra117.000314.

STAR★METHODS

KEY RESOURCES TABLE

REAGENT or RESOURCE	SOURCE	IDENTIFIER
Antibodies		
Parkin (phospho-Ser65) antibody	Biorbyt	Cat#: orb312554
Parkin (Prk8) Mouse mAb	Cell signaling	Cat#: 4211; RRID:AB_2159920
Total OXPHOS Rodent WB Antibody Cocktail	Abcam	Cat#: ab110413; RRID:AB_2629281
Alpha Tubulin Mouse Monoclonal Antibody	Proteintech	Cat#: 66031-1-Ig; RRID:AB_11042766
Anti-UBC13 Antibody (F-10)	Santa Cruz	Cat#: sc-376470; RRID:AB_11150503
VDAC	Proteintech	Cat#: 10866-1-AP; RRID:AB_2257153
Chemicals, peptides, and recombinant proteins		
Urolithin A (Mitopure)	Amazentis	N/A
Critical commercial assays		
V-PLEX Human CRP Kit	Meso Scale Discovery	Cat#: K151STD
V-PLEX Proinflammatory Panel 1 Human Kit	Meso Scale Discovery	Cat#: K15049D
QiaSymphony RNA extraction kit	Qiagen	Cat#: 931636
QIAsymphony DNA Mini kit	Qiagen	Cat#: 937236
Deposited data		
RNA-seq dataset	This study	GEO: GSE197273
Human reference genome NCBI Release 32 (GRCh38.p13)	Genome Reference Consortium	https://www.ncbi.nlm.nih.gov/grc/human
Oligonucleotides		
HSMTND1 Taqman Probe	This study	Custom made
HS18S Taqman Probe	This study	Custom made
Software and algorithms		
ImageJ-win64	NIH	https://imagej.nih.gov/ij/
GraphPad Prism 9.3.1	GraphPad Software	https://www.graphpad.com/
R, v. 4.0.3		https://cran.r-project.org/
DESeq2 v. 1.30.0	Love MI et al., 2004	https://bioconductor.org/packages/release/bioc/html/DESeq2.html
clusterProfiler, v. 3.18.0	Yu et al., 2012	https://bioconductor.org/packages/release/bioc/html/clusterProfiler.html
Other		
4–15% Mini-PROTEAN® TGX™ Precast Protein Gel	Biorad	Cat#: 4561086
Protease inhibitor cocktail	Thermofisher	Cat#: 78430
Phosphatase inhibitor cocktails	Thermofisher	Cat#: 78428
Transblot transfer	Biorad	Cat#: 1704156
10x TBST	Brunschwig	Cat#: SER42598-01
Non-fat dried milk	Applichem	Cat#: A0830
4x Laemmli Sample Buffer	Biorad	Cat#: 1610747

RESOURCE AVAILABILITY

Lead contact

Further information and requests for resources and reagents should be directed to and will be fulfilled by the lead contacts, Drs. Anurag Singh and Chris Rinsch (asingh@amazenis.com; contact@amazenis.com).

Materials availability

All unique/stable reagents generated in this study are available from the lead contacts, Drs. Anurag Singh and Chris Rinsch, with a completed Material Transfer Agreement.

Data and code availability

- RNA-seq data have been deposited at GEO (accession number: GSE197273).
- This study did not generate codes.
- Any additional information required to reanalyze the data reported in this paper is available from the lead contact upon request.

EXPERIMENTAL MODEL AND SUBJECT DETAILS

Trial design and study schedule

The study (ATLAS) is a randomized, double-blind, placebo-controlled study enrolling healthy, overweight, middle-aged subjects, who received UA (Mitopure™; Amazentis SA), orally for 4-months at the dosing of 500 mg (n = 29), 1,000 mg (n = 30) or the corresponding placebo (n = 29) as described in the CONSORT table (Figure 1). The study was approved by an independent private IRB (Advarra IRB) and by the Natural product division of Health Canada. Subjects were recruited at the clinical site (KGK Science, London, Ontario, Canada) via a participants database and through social media campaigns. Recruitment started in March 2018 and the last subject completed the study in August 2019. 253 subjects were screened in total of which n = 88 met all the study inclusion and exclusion criteria and were randomized. There were 4 study visits during the course of the trial. Screening visit (Visit 1) occurred up to 45 days prior to baseline visit (Day 0). At baseline (Visit 2) subjects performed the various study measures and were randomized into the different interventions. Subjects returned back to the clinic 2-months after study start (Day 60 ± 4; Visit 3) and 4-months at the end of the study duration (Day 120 ± 4; Visit 4). Recruited and randomized subjects' demographics are shown in Table S1. A total of n = 79 subjects completed the study and there were 9 drop-outs (2 each in placebo and 500mg UA intervention and 5 in 1000mg UA dose group). There were no major deviations of the clinical protocol. No concomitant diets/medications were reported. The Intent-to-treat (ITT) population consisted of all participants who were randomized and received the study product. The Per-protocol (PP) population consisted of all participants who showed 80% compliance to study products, completed all study visits and did not have any major study protocol deviations. All 88 subjects are included in the final analysis for the main clinical study endpoints (ITT analysis) (Figure S1). The n = 9 drop-outs and n = 5 poor compliant subjects were removed from the per protocol (PP) analysis (n = 74). The clinical study is registered in the registry www.clinicaltrials.gov (NCT03464500)and was conducted in accordance with the guidelines of the international council of harmonisation (ICH) for Good Clinical Practice (GCP) and the Declaration of Helsinki and follows the CONSORT reporting guidelines for randomized clinical trials

Inclusion and exclusion criteria

Study participants are aged ranged between 40 to 65 years and were above normal body weight (BMI between 25.0 and 34.9 kg/m^2). Subjects were sedentary and with low VO_{2max} (defined as less than <35 mL/kg/min via the ergometer prior to baseline) at the time of the study inclusion. Subjects agreed to avoid exercising 24-h prior to study visits and maintain low physical activity status for the duration of the trial. Subjects also should not have participated within the last year in any other clinical trial focused on physical or muscle performance. Subjects also agreed to refrain from consuming pomegranate juice or supplements and from taking other dietary interventions touted for muscle promoting benefits such as high-protein and CoQ10, Vitamin B3 and its precursors and L-carnitine. All subjects gave informed consent prior to study participation. Exclusion criteria included chronic smokers, history of alcohol abuse, those with chronic diseases that required medications (statins, blood thinners, steroid and thyroid medications), and participants who had either recently donated blood or did not like swallowing capsules. Subjects engaging in regular physical activity were also excluded in addition to those undergoing a weight-loss program. Subjects with previous metallic implants were also excluded.

METHOD DETAILS

Product intake and randomization

The investigational product was labeled according to the requirements of ICH-GCP guidelines and applicable local regulatory guidelines. Investigational product was randomized and coded by an unblinded person at the study CRO, who was not involved in data collection or analysis. A randomization schedule was created and provided to the Investigator indicating the order of randomization. Each participant was assigned a 6-digit randomization code according to the order of the randomization list generated using www.randomization.com. A "block randomized" list was created to ensure balance between the intervention groups during the randomization process. Primary packaging of the soft-gel was provided in blister packs. Packaging of the product was performed by PCI Pharma Services (4545 Assembly Drive, Rockford, IL, 61109, USA). For the purpose of the study, the daily dose of UA or placebo was delivered by secondary packaging into wallets containing an 8-days' supply, each day containing 4 softgels: (1) for Placebo daily dose: 4 Placebo softgels; (2) for 500mg UA daily dose: 2 UA soft-gels + 2 placebo softgels; (3) for 1000mg UA daily dose: 4 UA

softgels. Participants were instructed to take 4-soft-gel capsules of placebo, 500 mg, or 1,000 mg doses. These were provided in kits containing the blister packs. The blisters were packaged into 8-day (each day 4-softgels) wallet cards. Four (4) wallet cards (30 + 2 days' supply) were included in a final box/kit package for a month's worth of supply. Each participant received 2 monthly kits at start of the study and at the 2-month study visit. Four soft-gel capsules were to be taken in the morning before breakfast with water on an empty stomach on the day following randomization (Day 1). Subjects were instructed to take the soft-gel capsules one after another. The length of the intervention was four-months (120 days). If a participant forgot to take a dose, they were instructed to take the next dose as soon as they remembered. Participants were not to miss three consecutive days of product up to a maximum of three times during the course of the study or they were deemed non-complaint. The participants were instructed not to exceed the intake of four soft-gel capsules per day.

Compliance
Compliance was assessed by counting the returned unused test product at each visit. Compliance was calculated by determining the number of dosage units taken divided by the number of dosage units expected to have been taken multiplied by 100. Possible differences in compliance between the study groups at each visit and overall compliance were assessed by an analysis of variance (ANOVA).

Adverse event reporting
During the study, participants recorded any adverse effects in their diary. Any adverse events (AEs) were documented and classified according to the description, duration, intensity, frequency, and outcome. The qualified investigator assessed all AEs and decided on the causality. Intensity of AEs was graded on a three-point scale (mild, moderate, severe) and reported in detail in the study record. All adverse events were categorized by the MedDRA (Medical dictionary for regulatory activities) Version 20.1.

Data management and monitoring
Study data were processed in accordance with the principles of Good Clinical Practice. Data were acquired from source documentation and entered for each individual subject electronic case report form (eCRF) into a validated data management system (*Open Clinica Enterprise Version 3.11).* Data entry was completed by site personnel into the study database system. Reference ranges were provided to query each laboratory parameter used during the study to identify the out-of-range values. Prior to the database lock, every in a subject's eCRF was checked for completion of data entry. The data was monitored, validated and frozen prior to unblinding. The study blind was broken at the end of the study following blind database review and database lock approval. Emergency unblinding for safety reasons was not required during the conduct of the study. For study monitoring source documents were reviewed to ensure that all items had been completed and that the data provided are accurate and obtained as specified in the protocol. For each participant during the monitoring visits the following was reviewed to confirm that: Informed consent was obtained and documented; that enrolled participants fulfilled all inclusion criteria and did not meet any exclusion criteria; that AE/SAE reporting has been performed as applicable; study visits have been conducted as per protocol and information has been recorded in the appropriate place in the source document; and that the study product was being stored correctly and an accurate record of its dispensation to the study participants was being maintained.

Lower-body (muscle strength testing) using Biodex dynamometry
Lower body strength testing was performed using a Biodex isokinetic dynamometer (Wolf Orthopedic Biomechanics Lab, Western University, London, ON, Canada) as per the following protocol: The Biodex Multi-Joint System-3 dynamometer (Biodex Medical, Shirley, NY), its accompanying software, and methods used were similar to previously published protocols (King et al., 2008; Kean et al., 2010). During the testing session, the participants were seated with their back against a rigid backrest oriented 85° above the horizontal. The participant's pelvis and thigh were secured to the dynamometer using a seatbelt oriented diagonally across the anterior superior iliac spines and over the distal half of the quadriceps, respectively. The axis of rotation of the dynamometer lever arm was positioned coaxial with the lateral femoral epicondyle. The resistance pad was secured over the distal anterior one-third of the lower leg, above the malleoli. Participants performed 3 sets of 10 repetitions of reciprocal concentric isokinetic knee extension and flexion at an angular velocity of 60 deg/sec. Before testing, participants performed a 5-min warm-up on a stationary cycle ergometer at a low rate (50 rpm) and low workload (1 kP). Before each test, participants performed two submaximal (50–65%) repetitions to allow for familiarization with the testing method. Participants then performed five reciprocal concentric isokinetic contractions of knee extension and knee flexion with maximum effort. Maximum strength values were calculated as the mean of the 5 peak torque scores in Nm, and as the one maximum score in Nm, for knee extension and for knee flexion.

Upper-body (hand-grip) muscle strength evaluation using dynamometry
Hand-grip strength was tested using a Jamar dynamometer (Chicago, IL, USA) as a measure of upper body strength. The same clinical coordinator performed the dynamometry measurements for each subject at all visits. The clinical coordinator instructed the subject to hold the grip strength dynamometer in their non-dominant hand and place their elbow against their side. On cue, the subject squeezed the handle of the dynamometer as hard as possible. The clinical coordinator recorded the maximum resistance value in kilograms that the dynamometer recorded. This process was repeated three times in the non-dominant hand. An overall average was calculated.

Incremental sub-maximal exercise testing

The purpose and protocol of the test were outlined to the participant. Participants were informed that they may withdraw from the exercise at any point during the test. The subjects were attached to the metabolic cart (*cardio-Coach*). Resting V_{O2} and heart rate were measured are made for 1 min. Participant initially began cycling at a suggested cadence = 70 rpm for 3 min to accommodate the initial light-intensity power output. This was followed by incremental exercise: after the 3-min baseline cycling, participants continued cycling and the load increased by 100 g every 30s. Heart rate was monitored continuously throughout the protocol and rate of perceived exertion (RPE) was monitored every 2 min. Additional load was continued to be added until the final criteria had been achieved i.e., the participant was unable to maintain a cadence despite strong verbal encouragement; or maximal heart rate was >85% based on Karvonen's formula; or respiratory exchange ratio (RER) > 1.15; or a rating of perceived exertion on the Borg scale of 19 or 20; or an inability to continue. A graph was generated comparing heart rate (HR) vs. rate of oxygen consumption (V_{O2}) using participants' data from the V_{O2} submaximal procedure. A trendline of the data was used to extrapolate a participant's age corrected to predicted max heart rate which was used to predict V_{O2Max}.

Dual energy X-ray absorptiometry (DXA)

The DXA scan (GE Healthcare, Madison, WI, USA) was performed by trained imaging technicians at the study site. The procedure was explained to study participants. It was confirmed that participant did not have any internal metal implant from chin down and that participants had not performed a scan recently ($\leq$5-day) where a contrast medium was administered. Participant were asked to wear comfortable clothing and not wearing any garments that contained metal, zippers, etc. during the scan. Participants were asked to remove jewelry, removable dental appliances, eye glasses and any metal objects or clothing that potentially might interfere with the X-ray images. Participants were positioned on the table, making sure that they were positioned properly on their back within the appropriate scanner detectors. Participants were positioned supine on the table with their arms by their side and having their head about one inch inside the border of the scanner. Scanner was set up with all required data for the participant entered in a folder created for them. Participant were asked not to move while the scanner was running. Once the exam was complete, it was confirmed that all the necessary information and images have been acquired.

6-min walk test (6MWT)

A distance of 15 m was marked on the floor of an indoor hallway regulated for temperature and humidity, and markers placed at each end of the course. Participants were instructed on how to complete the test by a trained clinical coordinator. The test consisted of subject's walking the length of the course, pivoting briskly at the end and returning to the starting point. The subject's completed as many laps of the course as possible over 6 min. The clinical coordinator provided encouragement and time updates at 1-min intervals over the length of the 6-min. At the 6-min mark the subject were asked to stop where they were standing and the clinical coordinator calculated the total distance that was walked in meters.

Plasma collection

Blood samples were drawn from all the study participants at screening, and at the end of study visit from a participant's arm via venipuncture. Approximatively 4 mL of blood was collected in lavender EDTA tubes until vacuum was exhausted and blood ceased to flow. Tubes were gently inverted 8–10 times to disperse anticoagulant, labeled and centrifuged immediately at 2,500 rpm for 15 min at 25 °C. Each sample was aliquoted in labelled cryovials containing 500 μL of plasma each. Each aliquot was used for a different plasma biomarker to avoid extra freeze-thaw cycles. Volume used from each aliquot are: 150–300 μL for metabolomics; 200–500 μL for bioavailability assessment; 200–300 μL for plasma CRP and cytokines measurement.

Bioavailability assessment of UA

Plasma concentrations of UA and its metabolites, UA-glucuronide and UA-sulfate, were analyzed in plasma samples. UA levels in plasma were assessed before the start of the study intervention and following the last dose of the 4-month study duration for bioavailability assessments with a validated method as described in.[28] The limit of quantification was 5.00 pg mL−1 for UA in plasma and 5.00 ng mL−1 for UA-glucuronide and UA-sulfate in plasma. For mean value calculations, all values below the limit of quantification were set to zero.

Plasma metabolomics

Metabolomics of plasma was performed by Metabolon Inc. according to published methods.[65] Briefly, sample preparation was conducted using a proprietary series of organic and aqueous extractions to remove the protein fraction while allowing maximum recovery of small molecules. The extracted samples were split into equal parts for analysis on the gas chromatography–mass spectroscopy (GC-MS) and liquid chromatography–tandem mass spectroscopy (LC-MS/MS) platforms. For LC-MS/MS, samples were split in two aliquots that were either analyzed in positive (acidic solvent) or negative (basic solvent) ionization mode. GC-MS was performed on bis(trimethylsilyl) triflouroacetamide-derivatized samples in a 5% phenyl GC column.

Plasma CRP and cytokine measurements

Human plasma samples were used to measure levels of C-reactive protein (MSD V-Plex K151STD) and a panel of cytokines (Human Pro-inflammatory Panel 1 K15049D) following manufacturing instructions. Samples were analyzed in a blinded fashion using a

dilution of 1:2 for the Human V-Plex Proinflammatory Panel 1 and of 1:100 for the Human CRP MSD assay. Standard curve concentration points on each plate were used to confirm where the calculated LLOQ for a particular analyte lies in comparison to the published LLOQ.

Muscle biopsies procedure

Muscle biopsies were collected in fasting conditions from the *vastus lateralis* muscle of the right leg on Day 0 pre-dose and on Day 120 in subjects that agreed and gave consent to the procedure (n = 59). Participants refrained from NSAID use for a full week prior to procedure. Prior to collection, the process was explained to participants at the beginning of the visit, with allergies to either Coverplast adhesive bandage or anesthetic Xylocaine declared beforehand (Sterile gauze and paper tape were be used if an allergy to Coverplast existed, and the procedure stopped if there was an allergy to Xylocaine). Area on participant's right leg (lateral thigh) to be used for muscle biopsy was cleaned with an alcohol swab and shaved if needed. Intramuscular injection (*vastus lateralis*) of 2.5 mL of 2% Xylocaine with a BD eclipse 25G X 1 ½ needle and 3 mL syringe was done to an area proximal to biopsy collection to ensure the sample was free of anesthetic. A 5-min waiting period was observed to allow anesthetic to take effect before the muscle biopsy area was cleaned 3 times with Stanhexidine aqueous 2% with 4% IPA. These biopsies were needle biopsies (Bergstrom Biopsy Needle and in some procedures Bard Core Biopsy Needle), and always performed by a qualified medical doctor and always at the same location of the *vastus lateralis*. Considering the length of the needle, the depth of the collection was around 4–5 cm below the skin and therefore in the muscle. The passing of *fascia lata* was perceptible and taken as a confirmatory sign that the needle was in the skeletal muscle. Each sample was divided in three portions of approximately 5–15 mg that were aliquoted in 2mL Eppendorf safelock and snap frozen using liquid nitrogen.

mRNA extraction from muscle biopsies

One muscle biopsy portion was added in RNA-later containing 2mL Eppendorf tubes. RNA was extracted from muscle vastus lateralis tissue using automated extraction protocols on the QiaSymphony platform using the QiaSymphony RNA extraction kit (cat. 931636) following the QiaSymphony RNA handbook 10/2009 and appropriate SOPs. RNA is quantified by Agilent Fragment Analyzer. Quality control of all of the samples will be done on the Agilent Bioanalyzer. Only samples for which muscle biopsies were available both before (Day 1) and after (day 120) the supplementation were used for RNA extraction.

Library preparation and RNA-seq

Library preparation and was performed using the Strand-specific cDNA library. RNA samples were subjected to purification of poly-A containing mRNA molecules, fragmented mRNA fragmentation. Random primed cDNA synthesis (strand-specific) and adapter ligation and adapter specific PCR amplification was then performed. All libraries were used for subsequent RNA-seq analysis. RNA-seq run was performed using the Illumina HiSeq 4000 sequencing platform with single reads (1 × 50 bp) and 30 million reads (+/- 3%). All samples were randomized in the RNA-seq plates to avoid batch effects. FASTQ files were generated for each sample.

Gene expression analysis using RNA-seq

The quantification of mRNA from the RNA-seq FASTQ files was performed using Salmon, for both Day 1 (Baseline, BL) and Day 120 visits, from 18 Placebo, 18 UA 500 mg and 21 UA 1000 mg samples. Sample-wise quant.sf files containing raw transcript-level read estimates were read into R, v. 4.0.3 and were combined into a data matrix. Transcripts with very low total counts (< 10) across all samples were filtered out. The data was transformed using the variance stabilizing transformation (VST) method of R package DESeq2, v. 1.30.0.[66] Top 10,000 transcripts with the highest variance across all samples were used for principal component analysis (PCA) using DESeq2. Data transformation and PCA was also done separately for each treatment group. Based on the PCAs, probable outlier samples were excluded and new PCAs were plotted without these samples. The raw transcript-level read count estimates were read in R and summarized to gene-level counts based on the provided transcript and gene ID annotations using summarizeToGene function of R package tximport, v. 1.18.0. DESeqDataSetFromTximport function of DESeq2 was then used for constructing a DESeqDataSet object for DE analysis. Pre-filtering was applied before the DE analysis by excluding genes with <10 total counts across samples. Subset DE analysis was performed, contrasting Visit time D120 with baseline (BL) and by adjusting for the subject effect. The normalization and DE analysis was done separately for the three different treatment groups. Independent filtering option of DESeq2 was enabled (default), filtering out genes with very low counts and thus unlikely to show significant evidence. R package biomaRt. v. 2.46.0 was used for annotating the results with HGNC gene symbols, gene descriptions and gene biotypes. DESeq2-normalised expression values of all the samples in the given comparison were added to the result tables. Non-adjusted p value 0.05 was used to filter the results by statistical significance. Results were also generated using DESeq2 function lfcShrink that allows for the shrinkage of the log2 fold change (LFC) estimates toward zero when the information for a gene is low (such as in those cases with low counts or high dispersion values) but has little effect on genes with high counts. The shrinked log2FC values were subsequently used for visualisation and ranking the genes.

Gene set enrichment analysis (GSEA)

Gene set enrichment analysis (GSEA) was conducted using R package clusterProfiler, v. 3.18.0.[67] Enrichments of Gene Ontology (GO) Biological Process (BP), Molecular Function (MF) and Cellular Compartment (CC) terms were investigated. All the genes

subjected to the DE analysis and that passed the independent filtering of DEseq2 were ranked by shrunk log2 fold change values and used as input data for the analysis. Ensembl IDs of the genes were converted to Entrez IDs for the analysis using biomaRt, v. 2.46. Minimum and maximum genes et sizes were set to 15 and 500, respectively. The simplify function of clusterProfiler was used to reduce redundancy of the results. Briefly, GO terms with semantic similarity higher than 0.7 were treated as redundant terms, and a representative term was then selected by taking the term with smallest adjusted p value. The obtained enrichment results were then filtered to exclude those terms that had only one core enrichment gene and non-adjusted p value > 0.05. In order to adjust for the placebo effect, the GSEA results of the Low Dose and High Dose DEGs were filtered to exclude enriched terms (p value < 0.05) obtained from the GSEA of the Placebo DEGs. The top results were visualised as GSEA plots using the clusterProfiler functions gsea-plot2, dotplot and cnetplot. DE genes with non-adjusted p value < 0.05 were compared between the treatment groups using Venn diagrams. R packages VennDiagram, v. 1.6.20 and venn, v. 1.9 were used for generating the diagrams and extracting genes in each Venn section. Similar analysis was done for comparing the enriched GO terms (with p value < 0.05) from the GSEA, using the simplified results.

Muscle proteomics

Human muscle samples were homogenized and denatured using a urea-based proprietary denaturing buffer (Biognosys' Denature Buffer). Proteins were reduced and alkylated using Biognosys' Reduction and Alkylation Buffer. Digestion to peptides was carried out using trypsin (Promega, 1:50 protease to total protein ratio) per sample overnight at 37 °C. Peptides were desalted using a C18 MicroSpin plate (The Nest Group) and dried down using a SpeedVac system (Thermo Scientific™). Peptides were resuspended in 50 µL water containing 1% acetonitrile and 0.1% formic acid (FA) (Solvent A) and spiked with Biognosys' iRT kit calibration peptides. Peptide concentrations were determined using a UV/VIS Spectrometer (SPECTROstar Nano, BMG Labtech). For the generation of the spectral library, a pool was prepared by combining aliquots from all samples. Ammonium hydroxide was added to reach a pH value >10. The sample pool was fractionated using a Dionex UltiMate 3000 RS pump (Thermo Scientific) on an Acquity UPLC CSH C18 1.7 µm, 2.1 × 150 mm column (Waters). The gradient was 1%–40% solvent B in 20 min, solvents were A: 20 mM ammonium formate in water, B: acetonitrile. Fractions were taken every 30 s and sequentially pooled to 8 fractions, dried down and resuspended in Solvent A, and spiked with iRT kit calibration peptides. One microgram of peptides per sample or fraction was injected to an in-house packed reversed phase column (PicoFrit emitter with 75 µm inner diameter, 60 cm length and 10 µm tip from New Objective, packed with 1.7 µm Charged Surface Hybrid C18 particles from Waters) on a Thermo Scientific EASY-nLC™ 1,200 nano-liquid chromatography system connected to a Thermo Scientific Q Exactive™ HF-X mass spectrometer equipped with a Nanospray Flex™ Ion Source. LC solvents were A: 1% acetonitrile in water with 0.1% FA; B: 20% water in acetonitrile with 0.1% FA. The nonlinear LC gradient was 1–59% solvent B in 85 min followed by 59–90% B in 10 s, 90% B for 8 min, 90%–1% B in 10 s and 1% B for 5 min at 60 °C and a flow rate of 250 nL/min. For DDA LC-MS/MS measurements, fractions were analyzed using a modified TOP15 method from Kelstrup was used.[68] For DIA LC-MS/MS measurements a method consisted of one full range MS1 scan and 29 DIA segments was adopted from.[69] The spectral library was generated by analyzing DDA data with SpectroMine™, FDR on peptide and protein level was set to 1%. A human UniProt fasta database (*Homo sapiens*, 2020-07-01) was used for the search engine, allowing for 2 missed cleavages and variable modifications (N-term acetylation, methionine oxidation). DIA data were analyzed using Spectronaut™ Pulsar software (Biognosys). FDR was set to 1 %, data was filtered using row-based extraction. The assay library (protein inventory) was used for the analysis. The DIA measurements were normalized using local regression normalization. As for RNA-seq data, samples taken before and after treatment had been compared to measure changes in protein abundance due to the treatment. Differentially expressed proteins from the above-described comparisons were subjected to WikiPathways enrichment analysis using the R package clusterProfiler, v. 3.18.0. Genes coding for the differentially expressed proteins (DEPs) with positive fold-change and false discovery rate (FDR) < 0.25 were used for the analysis. DEP genes from the Placebo analysis were excluded in order to adjust for the placebo effect. The top results were visualised as using the clusterProfiler functions gseaplot2, dotplot and cnetplot. Venn diagrams showing the overlap of the WikiPathways enrichment results were generated using R packages VennDiagram, v. 1.6.20 and venn, v. 1.9. Pathways with adjusted p value ≤ 0.1 were used as input and lists of proteins in each Venn section were extracted.

Western blot analysis

Muscle tissues were lysed in denaturing buffer as described above and added protease and phosphatase inhibitor cocktails (Thermofisher, 78430 and 78428). Sample volume ranged between 100-300 µL. Samples were sonicated for 20 min using an ultra-sonic bath (Branson 1,510) speed, and centrifuged at 13.000 rpm at 4 °C for 20 min. Clear supernatants were collected and used to assess protein concentration by DC protein assay (Bio-Rad, 500-0112). Lysates were eluted in 5x Laemmli buffer (Biorad, 1610747). 15 µg of protein lysates for each sample were separated by SDS-PAGE (Biorad, 1610732) and transferred onto polyvinylidene difluoride membranes (Biorad, 17001917). Filters were washed in TBS + 0.05% Tween and blocked for 1 h with 5% Non-Fat milk. Membranes were stained with red Ponceau (Sigma, P7170) to stain total protein pool. The following primary antibodies were incubated overnight diluted in blocking buffer: UBE2N (SantaCruz, sc-376470, 1:3000), Tubulin (Proteintech, 10004185, 1:3000), phospho-Parkin S65 (Cell Signaling, #36866, 1:1000), Parkin (Cell Signaling, #4211, 1:1000), OXPHOS Antibody Cocktail (Abcam, ab110413, 1:2000),

VDAC (Proteintech, 10866-1-AP, 1:1000). After washings, the secondary antibody (goat-anti-mouse, Azure, AC2115, 1:5000) was incubated for 30 min. Antibody reactions detection were imaged using the GE Healthcare, ImageQuant LAS 500. Quantification of the protein band intensity was performed using Fiji.

mtDNA/nuDNA analysis

Muscle samples were incubated overnight in 360 µL of buffer proprietary ATL lysis buffer and 40 µL proteinase (Qiagen) at 55°C in a thermomixer set at 300 r.p.m. Cell debris was removed by centrifugation and 200 µL of clear lysates was placed in the QIAsymphony SP workstation (Qiagen). DNA was extracted with the QIAsymphony DNA Mini kit (Qiagen, catalogue no. 937236) following the manufacturer's procedures. Quantitative PCR was performed on the Fluidigm Biomark system following the Fluidigm Specific Target Amplification Quick Reference (Fluidigm). Samples were loaded as technical triplicates. The real-time PCR data were analysed using the Linear Derivative baseline correction and User (detector) Ct threshold method on the latest version of the Fluidigm Biomark software (v.4.1.3). Quantification of mtDNA was performed using two customized Taqman assays targeted against a nuDNA sequence (18S) and a conserved region of mtDNA (MTND1). Relative mtDNA copy number was determined comparing MTND1 to 18S signal. qPCR data quality control was performed and samples with low DNA sample concentration or low sample purity were discarded. These criteria were defined before starting the analysis of the raw data. Sample belonging to 4 subjects (2 placebo and 2 UA 1000 mg) did not meet the QC requirements and were excluded from the analysis

QUANTIFICATION AND STATISTICAL ANALYSIS

Clinical data

A total of three analytical populations are defined for all summaries and analyses. Every participant who meets the population criteria specified below were classified in the designated population: Intent-to-Treat (ITT), per protocol (PP) and safety population. The ITT population consisted of all participants who received either product, and on whom any post-randomization efficacy/effectiveness information was available. The PP population consists of all participants who consumed at least 80% of treatment or placebo doses, did not have any major protocol violations and completed all study visits and procedures connected with measurement of the primary variable. The safety population consisted of all participants who received any amount of either product, and on whom any post-randomization safety information was available. As this was an exploratory, proof-of-concept study designed to identify the endpoint with the most responsive signal with supplementation, all endpoints were considered exploratory. Still to ensure an appropriate sample size to identify the signal, the following sample size estimates were utilized for the study utilizing exercise intervention studies in similar populations: a) two-sided testing with overall alpha equal to 0.05. b) 80% power to detect a significant difference during submaximal exercise test (peak power output), and c) a 20% attrition rate from enrollment to final, post-baseline measurement. The sample size was calculated on the basis of an independent Student's t-test assuming a dose response with the active treatment. 87 subjects were calculated to be required for a 3-group study to have an 80% power with a 0.05 alpha and 20% attrition rate. All statistical testing used were two-sided and performed at the 0.05 significance level. Tests were declared statistically significant if the calculated p value was ≤ 0.05. The endpoints were analyzed for both ITT and PP populations All analyses were performed using R Statistical Package version 3.5.3 (R Core Team, 2019). For summaries of continuous variables, the arithmetic mean, standard deviation, median and minimum-maximum range were presented to two decimal places. Possible differences between groups at baseline was assessed by an analysis of variance (ANOVA). In the case of a significant between group difference, pairwise comparisons were conducted with alpha adjustment using Tukey's HSD. For each group, change in parameters between visits were assessed using a paired Student's t-test or Wilcoxon Signed-Rank test. Possible differences between groups for change in parameters were assessed by a linear or repeated mixed-effects models, controlling for the baseline value in the model.

Plasma biomarkers

Change in plasma levels of acylcarnitines was assessed using repeated Measures ANOVA to analyze the data. Missing values, if any, were imputed with the observed minimum for that particular compound. The statistical analyses were performed on natural log-transformed data. For plasma CPR and cytokines, post baseline markers were analyzed in the Log10 scale using an analysis of covariance (ANCOVA), correcting for baseline value and treatment arm. In case of observed value below the limit of detection, left censoring was applied. Point estimate, 80% and 95% confidence intervals were extracted from the ANCOVA model. No correction for multiplicity testing was applied. Analysis was performed using R version 4.0.3

RNA-seq

Differential gene expression (DGE) was calculated from RNA-seq data within each treatment group comparing D120 to D1 (baseline, BL) using a Wald-test. Genes sets were taken from the MSIGDB C5 GO collection. Gene sets with adjusted p.value < 0.1 were selected. Gene sets significantly enriched in the both the treatments and placebo groups were considered are false positive hits and removed from the analysis.

Proteomics

For testing of differential protein abundance, log2 peptide intensity ratios between replicate pairs for each protein were analyzed using a one sample t-test ($\mu = 0$). p-values were corrected for overall FDR using the q-value approach.

mtDNA/nuDNA

The mtDNA/nuDNA ratio calculated according to the following equation:

$$\frac{mtDNA}{nuDNA} ratio = 2^{-\Delta\Delta Ct}$$

$$\Delta\Delta Ct = \left(\mu Ct_{MTND1(D120)} - \mu Ct_{18s(D120)}\right) - \left(\mu Ct_{MTND1(BL)} - \mu Ct_{18s(BL)}\right)$$

Where:

μCt_{MTND1} is the mean threshold cycle (Ct) of the technical triplicate of MTND1

μCt_{18s} is the the mean Ct of the technical triplicate of 18S

The effect of treatment on mtDNA/nuDNA ratio was tested using a type II analysis of variance (Wald test) at baseline (to test for proper randomization) and over time (D120 – BL) after correction for multiple testing. A post-hoc analysis on the individual treatment group comparison was conducted when the effect of treatment was significant.